Genetic Evidence Links the ASTRA Protein Chaperone Component Tti2 to the SAGA Transcription Factor Tra1

Julie Genereaux,* Stephanie Kvas,* Dominik Dobransky,* Jim Karagiannis,† Gregory B. Gloor,*
and Christopher J. Brandl*,1

*Department of Biochemistry, Schulich School of Medicine and Dentistry, University of Western Ontario, London, Ontario, Canada
N6A5C1 and †Department of Biology, University of Western Ontario, London, Ontario, Canada N6A 5B7

ABSTRACT Tra1 is a 3744-residue component of the *Saccharomyces cerevisiae* SAGA, NuA4, and ASTRA complexes. Tra1 contains essential C-terminal PI3K and FATC domains, but unlike other PIKK (phosphoinositide three-kinase–related kinase) family members, lacks kinase activity. To analyze functions of the FATC domain, we selected for suppressors of *tra1-F3744A*, an allele that results in slow growth under numerous conditions of stress. Two alleles of *TTI2*, *tti2-F328S* and *tti2-I336F*, acted in a partially dominant fashion to suppress the growth-related phenotypes associated with *tra1-F3744A* as well as its resulting defects in transcription. *tti2-F328S* suppressed an additional FATC domain mutation (*tra1-L3733A*), but not a mutation in the PI3K domain or deletions of SAGA or NuA4 components. We find eGFP-tagged Tti2 distributed throughout the cell. Tti2 is a component of the ASTRA complex, and in mammalian cells associates with molecular chaperones in complex with Tti1 and Tel2. Consistent with this finding, Tra1 levels are reduced in a strain with a temperature-sensitive allele of *tel2*. Further agreeing with a possible role for Tti2 in the folding or stabilization of Tra1, *tra1-F3744A* was mislocalized to the cytoplasm, particularly under conditions of stress. Since an intragenic mutation of *tra1-R3590I* also suppressed F3744A, we propose that Tti2 is required for the folding/stability of the C-terminal FATC and PI3K domains of Tra1 into their functionally active form.

Tra1 and its human homolog TRRAP are members of the PIKK (phosphoinositide three-kinase–related kinase) family of proteins. The family also includes the key cellular regulators ataxia telangiectasia mutated (ATM), ATM and Rad3-related (ATR), DNA-dependent protein kinase catalytic subunit (DNA-PKcs), mammalian target of rapamycin (mTOR), and suppressor with morphological effect on genitalia family member (SMG-1), many with yeast equivalents (Abraham 2004; Lovejoy and Cortez 2009). Tra1 is essential for viability in *Saccharomyces cerevisiae* and a major constituent of the multisubunit SAGA and NuA4 transcriptional regulatory complexes (Grant *et al.* 1998; Saleh *et al.* 1998; Allard *et al.* 1999). SAGA and NuA4 have been well studied

with regard to their functions, playing roles in multiple aspects of gene regulation and DNA repair (Doyon and Cote 2004; Rodriguez-Navarro 2009; Koutelou *et al.* 2010). Both possess histone acetyltransferase activity, the catalytic subunits being Gcn5 and Esa1 for SAGA and NuA4, respectively (reviewed in Roth *et al.* 2001). SAGA contains additional modules, critical for regulation, that function in the deubiquitylation of histone H2B (Henry *et al.* 2003) and interaction with the TATA binding protein (Dudley *et al.* 1999; Mohibullah and Hahn 2008). Structural data indicate that Tra1 comprises a separate module in SAGA and NuA4 (Wu *et al.* 2004; Chittuluro *et al.* 2011). The position of Tra1 in these complexes is not indicative of a scaffold function, a result consistent with Tra1 not being required for stability of *Schizosaccharomyces pombe* SAGA (Helmlinger *et al.* 2011). This function is primarily ascribed to Spt7 for SAGA and Eaf1 for NuA4 (Sterner *et al.* 1999; Auger *et al.* 2008). TRRAP was first identified through its interactions with the transcription factors c-myc and E2F (McMahon *et al.* 1998). Similarly Tra1 interacts with yeast transcription factors, targeting SAGA and NuA4 to specific promoters (Brown

et al. 2001; Bhaumik et al. 2004; Fishburn et al. 2005; Reeves and Hahn 2005). Independent functions for Tra1 likely also exist since Helmlinger et al. (2011) found that in S. pombe, deletion of the SAGA-specific molecule spTra1 results in changes in gene expression distinct from loss of other SAGA subunits.

On the basis of the association of the members in a series of immunoprecipitation experiments, Shevchenko et al. (2008) identified Tra1 in a novel complex they termed ASTRA (ASsembly of Tel, Rvb, and Atm-like kinase). The components of ASTRA are encoded by essential genes in S. cerevisiae and include: Tra1, Rvb1, Rvb2, Tel2, Tti1, Tti2, and Asa1. In S. pombe, Tra1 but not Tra2, is found in ASTRA (Helmlinger et al. 2011). Rvb1 and Rvb2 are components of multiple regulatory complexes (in S. cerevisiae the Ino80, Swr1, and R2TP complexes), likely in multimeric form (Jha and Dutta 2009; Huen et al. 2010). Both belong to the AAA$^+$ (ATPase associated with diverse cellular activities) family of ATP binding proteins. Lustig and Petes (1986) identified TEL2 in S. cerevisiae through mutations that result in generation-dependent telomere shortening. The association of mammalian and fission yeast Tel2 with several PIKK family members suggested a broader role (Hayashi et al. 2007; Takai et al. 2007). Tti2 and Tti1 were implicated in Tel2-dependent processes on the basis of their mutual association in yeast and mammalian cells (Hayashi et al. 2007; Takai et al. 2007, 2010; Hurov et al, 2010; Kaizuka et al. 2010). At least one role for Tel2, Tti1, and Tti2 (TTT complex, Hurov et al. 2010) is likely in the folding/maturation of PIKK proteins since they affect the steady-state levels and bind newly synthesized PIKK molecules (Takai et al. 2007, 2010; Horejsí et al. 2010; Hurov et al. 2010; Kaizuka et al. 2010). Furthermore, the TTT complex is functionally associated with Hsp90, Hsp70, Hsp40, and the R2TP/prefoldin-like complex (Horejsí et al. 2010; Takai et al. 2010). In a recent study of essential genes, tti1 and asa1 were implicated in chromosome instability (Stirling et al. 2011). Stirling et al. (2011) also demonstrate that knockdown mutants of these genes, as well as tti2 and tel2, result in telomere shortening and a reduction in Tor1 protein levels.

The PIKK family members are large proteins (3744 residues for Tra1), characterized by a C-terminally positioned domain that resembles the phosphatidylinositol-3-kinases (PI3K; Lempiäinen and Halazonetis 2009). Unlike the other PIKK family members, Tra1/TRRAP lack kinase activity (McMahon et al. 1998; Saleh et al. 1998). Despite this, altering residues that parallel key regions of the kinase members affect Tra1 function (Mutiu et al. 2007). Interestingly one of these mutations, tra1-SRR$_{3413}$ results in age-dependent telomere shortening. On the N-terminal side of the PI3K domain is a FAT (FRAP-ATM-TRRAP) domain that consists largely of HEAT (Huntington, elongation factor 3, PR65/A, TOR) and TPR (tetratricopeptide) repeats; indeed much of the protein is likely helical (Bosotti et al. 2000; Perry and Kleckner 2003; Sibandi et al. 2010; Knutson and Hahn 2011). To the C-terminal side of the PI3K domain is the less highly conserved PRD (PIKK regulatory domain), the site of acetylation of ATM by TIP60 (Sun et al. 2005; for a linear schematic of the domains see Lempiäinen and Halazonetis 2009).

At the extreme C terminus of the PIKK molecules is the 30–35 residue FATC domain (FAT C-terminal; Bosotti et al. 2000); the conservation of the domain is evident from the finding that some FATC domains can be exchanged without loss of function (Jiang et al. 2006). Addition of as little as a single glycine to the C terminus of Tra1 results in loss of viability (Hoke et al. 2010). Other FATC mutations in Tra1 cause growth defects, such as temperature sensitivity and slow growth on media containing ethanol, Calcofluor white, or rapamycin. The FATC domain is similarly important for the other PIKK family members (Priestley et al. 1998; Beamish et al. 2000; Takahashi et al. 2000; Sun et al. 2005). Of note, the parallel mutation to L3733A of Tra1 results in a dramatic loss in the kinase activity of SMG-1 (Morita et al. 2007). The structure of the isolated FATC domain of S. cerevisiae Tor1 has been determined (Dames et al. 2005). It is largely helical in structure with a C-terminal loop held in place by a disulphide linkage. While the helical structure is likely conserved, the absence of the cysteines in the other FATC domains suggests the loop is not. FATC domains are proposed to serve as the target site for protein interactions. In a two-hybrid analysis the FATC domain of Mec1, the S. cerevisiae homolog of ATR, was required for association with the RPA components Rfa1 and Rfa2 (Nakada et al. 2005). Similarly the FATC domain of ATM was shown to interact with Tip60 (Sun et al. 2005); however, a recent report suggests that this is indirect (Sun et al. 2010). Lempiäinen and Halazonetis (2009) speculate that the FATC and PRD domains regulate the kinase domain through interactions with the activation loop similar to the helical domains of the PI3 kinases.

We selected for suppressors of the temperature and ethanol sensitivity of tra1-F3744A with the goal of identifying roles for the FATC domain. Two mutations in tti2 were found in independent selections as partially dominant suppressors of the growth-related phenotypes and transcriptional changes caused by tra1-F3744A. tti2-F328S suppressed a second FATC mutation but not a mutation within the PI3K domain or deletion of SAGA or NuA4 components. Consistent with the documented role of the TTT complex (Takai et al. 2007, 2010; Horejsí et al. 2010; Hurov et al. 2010; Kaizuka et al. 2010), Tra1 levels were reduced in a strain temperature sensitive for Tel2, and an increased level of cytoplasmic Tra1-F3744A was reversed by tti2-F328S. We predict that the basis for the suppression results from Tti2 having a role in the formation, stability, and/or localization of active Tra1. Our finding that an intragenic mutation of arginine 3590 to isoleucine within the putative activation loop of Tra1 also suppresses the F3744A mutation supports the models of Lempiäinen and Halazonetis (2009) and Sturgill and Hall (2009) that folding of the PIKK molecules involves the interaction of FATC and PI3K domains.

Materials and Methods

Yeast strains and growth

Yeast strains, listed in Table 1, are derivatives of BY4741 and BY4742 (Winzeler and Davis 1997). *HIS3*-linked *tra1* strains, wild-type *TRA1* (CY4353), *tra1-L3733A* (CY4057 and CY4103) and *tra1-F3744A* (CY4350 and CY4351), are described in Hoke *et al.* (2010). The *HIS3* allele marking these alleles is placed at the *Bst*BI site of YHR100C/*GEP4*, 11 codons from the C terminus. A copy of YHR100C on YCplac111 or YCplac33 was present in each of these strains to ensure its functionality. Diploid strains containing one Flag[5]-tagged *TRA1* allele marked with *URA3* (CY4398) containing *TRA1-HIS3* (CY4419) or *tra1-F3744A-HIS3* (CY4421) were similarly constructed as were N-terminally eGFP-tagged *tra1* strains. The haploid *tra1-F3744A* strain (CY5524) containing 5′-*URA3*-Flag[5] and linked to 3′ *HIS3* was obtained after sporulation. CY5639 and CY5640 containing *Flag[5]-tra1-R3590I* and *Flag[5]-tra1-3590I, F3744A* were also generated after integration into CY4398 and sporulation. The *tra1-F3744A tti2-F328S* (CY5567 and CY5669) and *tra1-F3744A tti2-I336F* (CY5843) double mutant strains were obtained in the selection process described below. The *tti2-F328S* strain CY5665 was obtained after crossing CY5667 with BY4742. Double mutants with *ada2Δ0* (CY5876), *eaf3Δ0* (CY5916), and *eaf7Δ0* (CY5917) were generated after mating CY5667 with the consortium knockout strains (BY4842, BY7143, and BY4940 obtained from Open Biosystems) and screening Kan[r]-resistant spore colonies for the *tti2* allele by sequencing of PCR products. The *tti2-F328S* double mutant with *tra1-L3733A* was obtained after a cross with CY4103. The *spt7::LEU2* deletion strain used for double mutant analysis (CY5873) was created after five backcrosses of FY1093 (kindly provided by Fred Winston) with BY4741. RFP-tagged strains in the EY0987 background (*MATα his3Δ1 lys2Δ0 ura3Δ0*; Huh *et al.* 2003) were kindly provided by Peter Arvidson. Heterozygous diploid strains containing an RFP-tagged allele and *eGFP-tra1-F3744A* were made by mating the EY0987 derivatives with CY6018. CY6146 and CY6148 containing *tra1-F3744A* and either *tti2-1* (Stirling *et al.* 2011) or *tel2-15* (Grandin *et al.* 2012), both temperature-sensitive alleles, were produced after mating of CY4350 with PSY561 or PSY42 (kindly provided by Peter Stirling), respectively, and sporulation. CY6141 with Flag[5]-tagged Tra1 and *tel2-15* were produced from a cross of PSY43 with CY5919. CY6137 was derived after a cross of CY2222 and CY5665.

Growth comparisons were performed on YP media containing 2% glucose (YPD) selective plates after 3–5 days at 30° unless stated otherwise. Standard concentrations used for the selections were: 0.03% methyl methanesulfonate (Sigma-Aldrich), 7.5 μg/ml Calcofluor white (Sigma-Aldrich), 1.0 μg/ml tunicamycin (Sigma-Aldrich), 6% ethanol, 60 μg/ml brefeldin (LC Laboratories, Woburn MA), 1.2 M NaCl, 1.0 M sorbitol, 20 μg/ml geneticin (Sigma-Aldrich), 1.0 μg/ml staurosporine (LC Laboratories), 1.0 μg/ml phleomycin (Sigma-Aldrich), and 1 ng/ml rapamycin (LC Laboratories).

DNA molecules

Promoter-*lacZ* fusions cloned as *his3-lacZ* fusions into the *LEU2* centromeric plasmid YCp87 and have been described (Brandl *et al.* 1993; Mutiu *et al.* 2007; Hoke *et al.* 2010). Molecules for integrating *tra1* alleles linked to *HIS3* are described in Hoke *et al.* (2010). Integrative vectors to generate Flag[5] and eGFP fusions of Tra1 were constructed in cassettes using as the base a molecule synthesized by Integrative DNA Technologies. This molecule pCB2143 (see Supporting Information, Figure S1), cloned into pTZ19 (lacking the polylinker *Hin*dIII site) as a *Sph*I–*Bam*HI fragment contains an *Sph*I site at −549 relative to the translational start site of *TRA1*, a *Hin*dIII site inserted at −351, the sequence ACAA AATGTCAGGATCC surrounding the translational start and a *Bam*HI–*Sal*I fragment encoding a Flag[5] tag followed by a *Not*I site in the alanine frame, to which the coding region of *TRA1* to the *Kpn*1 site is added (Saleh *et al.* 1998). Inserted into this is the 1.1-kbp *Hin*dIII genomic fragment encoding *URA3*. The integrative plasmid was switched to eGFP by the replacement of the Flag cassette with a *Bam*HI–*Not*1 cassette encoding eGFP (Hoke *et al.* 2008a). Myc[9]-tagged *TTI2* and *tti2-F328S* were expressed from the *DED1* promoter in YCplac111 by inserting a *Not*–*Sst*I fragment amplified from genomic DNA using oligoncleotides 5693-1 and 5693-2 (Table 2) downstream of the *DED1* promoter-myc[9] cassette (Hoke *et al.* 2010). N-terminally eGFP-tagged *TTI2* was expressed from the *DED1* promoter on YCplac33 (Hoke *et al.* 2008a). pYHR100C/*GEP4* genomic DNA was inserted into YCplac111 or YCplac33 as a *Bam*HI–*Eco*RI fragment after PCR with oligonucleotides 4966-1 and 4966-2.

Selection of suppressor strains

CY4350 containing YCplac111-YHR100C was grown to stationary phase in YPD. A total of 10 μl of culture, ∼2 million cells, was plated onto YPD and UV irradiated at a wavelength of 302 nm for 10 sec. Survival was ∼10%. Colonies growing at 37° were colony purified under nonselective conditions and reanalyzed for growth at 37° and on YPD plates containing 6% ethanol. The suppressor strains were crossed with the *URA3*-tagged *tra1-F3744A* strain, CY5928, to determine linkage of the suppressor with *tra1-F3744A*. One strain had an unlinked suppressor mutation that segregated in a 2:2 fashion. A *MATα* spore colony was backcrossed with CY4350 nine times at each stage selecting for temperature and ethanol-resistant spore colonies. The final isolate was named CY5667. This was sent for genomic sequencing as described below. The *tti2* mutations were verified after isolation of genomic DNA, PCR with oligonucleotides 6061-1 and 5693-2, and sequencing of the PCR product using 6061-1 as primer. The selection was repeated independently on three plates using an initial selection at 35° with 4% ethanol. Again one unlinked suppressor mutation was obtained. This was backcrossed seven times with CY4351 with the resulting strain called CY5843. The *tti2* allele was sequenced after PCR with oligonucleotides 5693-1 and 5693-2 using PWO

Table 1 Strains used in this study

Strain	Genotype	Reference
BY4743	MATa/α his3Δ1/his3Δ1 leu2Δ0/leu2Δ0 LYS2/lys2Δ0 met15Δ0/MET15 ura3Δ0/ura3Δ0	Winzeler and Davis (1997)
BY4741	MATa ura3Δ0 met15Δ0 his3Δ0 leu2Δ0	Winzeler and Davis (1997)
BY4742	MATα ura3Δ0 lys2Δ0 his3Δ0 leu2Δ0	Winzeler and Davis (1997)
BY2940	Isogenic to BY4741 except eaf7::KanMX	Winzeler and Davis (1997)
BY4282	Isogenic to BY4741 except ada2::KanMX	Winzeler and Davis (1997)
BY7143	Isogenic to BY4741 except eaf3::KanMX	Winzeler and Davis (1997)
FY1093	MATa spt7-402::LEU2 his4-917- lys2-173R2 leu2-1 ura3-52 trp1-63 ade8	Gansheroff et al. (1995)
CY2222	MATα can1Δ::STE2pr-SpHIS5 lyp1Δ his3Δ1 leu2Δ0 ura3Δ0 met10 LYS2+ tra1-SRR3413-URA3	Hoke et al. (2008a)
CY4398	Isogenic to BY4743 except TRA1/URA3-Flag⁵-TRA1	This work
CY4057	MATa ura3Δ0 his3Δ0 leu2Δ0 tra1-L3733A-HIS3	Hoke et al. (2010)
CY4103	MATa ura3Δ0 his3Δ0 leu2Δ0 tra1-L3733A-HIS3	Hoke et al. (2010)
CY4350	MATa ura3Δ0 his3Δ0 leu2Δ0 tra1-F3744A-HIS3	Hoke et al. (2010)
CY4351	MATα ura3Δ0 his3Δ0 leu2Δ0 tra1-F3744A-HIS3	Hoke et al. (2010)
CY4353	MATa ura3Δ0 his3Δ0 leu2Δ0 TRA1-HIS3	Hoke et al. (2010)
CY4419	Isogenic to BY4743 except TRA1/URA3-Flag⁵-TRA1-HIS3	This work
CY4421	Isogenic to BY4743 except TRA1/URA3-Flag⁵-tra1-F3744A-HIS3	This work
CY5524	MATa ura3Δ0 his3Δ0 leu2Δ0 URA3-Flag⁵-tra1-F3744A-HIS3 tti2-F328S	This work
CY5639	MATα ura3Δ0 his3Δ0 leu2Δ0 URA3-Flag⁵-tra1-R3590I-HIS3	This work
CY5640	MATa ura3Δ0 his3Δ0 leu2Δ0 tra1-R3590I, F3744A-HIS3	This work
CY5665	MATa ura3Δ0 his3Δ0 leu2Δ0 tti2-F328S	This work
CY5667	MATα ura3Δ0 his3Δ0 leu2Δ0 tra1-F3744A-HIS3 tti2-F328S	This work
CY5669	MATa ura3Δ0 his3Δ0 leu2Δ0 tra1-F3744A-HIS3 tti2-F328S	This work
CY5843	MATα ura3Δ0 his3Δ0 leu2Δ0 tra1-F3744A-HIS3 tti2-I336F	This work
CY5873	MATα ura3Δ0 his3Δ0 leu2Δ0 spt7-402::LEU2	This work
CY5876	MATa ura3Δ0 his3Δ0 leu2Δ0 tti2-F328S ada2::KanMX	This work
CY5912	Diploid of CY5667 x CY5524	This work
CY5915	MATα ura3Δ0 his3Δ0 leu2Δ0 tti2-F328S spt7-402::LEU2	This work
CY5916	MATa ura3Δ0 his3Δ0 leu2Δ0 tti2-F328S eaf3::KanMX	This work
CY5917	MATa ura3Δ0 his3Δ0 leu2Δ0 tti2-F328S eaf7::KanMX	This work
CY5919	MATα ura3Δ0 his3Δ0 leu2Δ0 URA3-Flag⁵-TRA1	This work
CY5920	MATα ura3Δ0 his3Δ0 leu2Δ0 URA3-Flag⁵-TRA1-HIS3	This work
CY5928	MATα ura3Δ0 his3Δ0 leu2Δ0 URA3-Flag⁵-tra1-F3744A-HIS3	This work
CY5998	Isogenic to BY4742 except URA3-eGFP-TRA1	This work
CY5999	MATα ura3Δ0 his3Δ0 leu2Δ0 tti2-F328S URA3-eGFP-tra1-F3744A-HIS3	This work
CY6016	MATα ura3Δ0 his3Δ0 leu2Δ0 URA3-eGFP-tra1-F3744A-HIS3	This work
CY6018	MATa ura3Δ0 his3Δ0 leu2Δ0 URA3-eGFP-tra1-F3744A-HIS3	This work
CY6025	Diploid of CY6016 x BY4741	This work
CY6029	Diploid of CY5998 x BY4741	This work
CY6063	Diploid of CY5999 x BY4741	This work
CY6072	MATα ura3Δ0 his3Δ0 leu2Δ0 URA3-Flag⁵-TRA1 YCplac111-TTI2	This work
CY6074	MATα ura3Δ0 his3Δ0 leu2Δ0 URA3-Flag⁵-tra1-F3744A-HIS3 YCplac111-TTI2	This work
CY6083	MATα ura3Δ0 his3Δ0 leu2Δ0 URA3-Flag⁵-tra1-F3744A-HIS3 YCplac111-tti2-F328S	This work
CY6137	MATα his3Δ1 leu2Δ0 ura3Δ0 tra1-SRR3413-URA3 tti2-F328S	This work
CY6141	MATα ura3Δ0 his3Δ0 leu2Δ0 URA3-Flag⁵-TRA1 tel2-15::KanMX	This work
QY204	MATa his3Δ200 trp1Δ63 ura3-52 leu2Δ1 lys2-126δ	Nourani et al. (2001)
QY202	MATa his3Δ200 trp1Δ63 ura3-52 leu2Δ1 lys2-126δ yng2:: KanMX	Nourani et al. (2001)
PSY36	MATa leu2Δ0 his3Δ0 lys2Δ0 asa1-1::URA3	Stirling et al. (2011)
PSY42	MATa ura3Δ0 leu2Δ0 his3Δ0 lys2Δ0 tel2-15::KanMX	Stirling et al. (2011)
PSY43	MATa ura3Δ0 leu2Δ0 his3Δ0 lys2Δ0 tel2-15::KanMX	Stirling et al. (2011)
PSY561	MATα leu2Δ0 his3Δ0 tti2-1::URA3	Stirling et al. (2011)
PSY625	MATα leu2Δ0 his3Δ0 lys2Δ0 tti1-1::URA3	Stirling et al. (2011)

polymerase (Roche Applied Science) and cloning of the resulting PCR product in pUC18.

Genomic sequence analysis

Three genomic DNAs were prepared, two strains containing the suppressor from independent tetrads and a control strain lacking the suppressor from the same tetrad as CY5667. Genomic DNA was prepared from 10 ml of lyticase-treated cells (Ausubel et al. 1988). Removal of RNA was verified by gel electrophoresis. Approximately 5 μg of DNA from each sample was sent to the Centre for Applied Genomics (Toronto, Ontario) for DNA library construction and next-generation sequencing using paired-end reads with the Applied Biosystems SOLiD 4.0 platform. The S. cerevisiae genome sequence was downloaded from the Saccharomyces Genome Database (SGD; http://www.yeastgenome.org) on March 24, 2011. Custom bash and Perl scripts were written for the sequencing analysis. The program Bowtie (Langmead et al. 2009),

Table 2 Oligonucleotides used in this study

Name	Sequence (5′–3′)	Description
4966-1	CGGGATCCAGAGCCACCTTCGGAGTA	YHR100C
4966-2	TTTGAATTCAACACCTACAGTCAC	
5693-1	ATAAGAATGCGGCCGCAATGACGGCCGTAACTGATATC	TTI2
5693-2	ATACGAGCTCTGCATTTGTCTGTGTCTGTGT	
6061-1	CCGGATCCATACTGAGACTTCAAAGAGAAGG	
5583-1	GTATCGATTCATTTAGAGATTGC	PHO5
5583-2	ATCCGAAAGTTGTATTCAACAAG	
5927-1	GGACAGACAACTTTGAAGATAAAG	PGK1
5927-2	GAATCGTGTGACAACAACAGCGTG	

allowing up to three mismatches per read, was used to map the colorspace reads to each chromosome of the yeast genome and obtain mapped reads in SAM format (Sequence Alignment/Map; Li *et al.* 2009). The variant call format (VCF) from SAMtools (Li *et al.* 2009) was used to obtain a raw list of polymorphisms from the mapped reads. Those reads with a Phred quality score <20 were eliminated to obtain a filtered list of polymorphisms. A custom Perl script was written to account for the polymorphisms found in wild-type samples. We do note that ∼5% of the *TTI2* reads for the suppressor strains were wild type, not containing the F328S codon. We believe these represent errors in the reading or synthesis of the barcodes on the 14 other yeast sequences in the lane.

β-Galactosidase assays

Yeast strains containing *lacZ*-promoter fusions were grown to stationary phase in media lacking leucine. Assays with *PHO5-lacZ* in media depleted of phosphate, and *HIS4-lacZ* in media lacking histidine were performed as described in Mutiu *et al.* (2007), *GAL10-lacZ* in media containing 2% galactose as the carbon source in Brandl *et al.* (1993), and for *RPL35a-lacZ* in YPD as described by Hoke *et al.* (2010). O-nitrophenol-β-D-galactosidase was used as substrate and values normalized to cell density.

Western blotting

Western blotting was performed using PVDF membranes and anti-Flag (M2; Sigma-Aldrich) or anti-Myc (9E10; Sigma-Aldrich) antibodies as described by Mutiu *et al.* (2007) or Hoke *et al.* (2010).

Chromatin immunoprecipitation assays

ChIP assays using anti-H3 (Abcam; ab1791), anti-AcH4 K8 (ab1760) and anti-AcH3 K18 (ab1191) were performed as described by Mutiu *et al.* (2007). Input chromatin for the immunoprecipitations was prepared from yeast strains CY4353, CY4350, and CY5667, and normalized by PCR analysis of serial dilutions using oligonucleotides 5583-1 and 5583-2 to the *PHO5* promoter. Agarose gels were stained with ethidium bromide and bands quantified using AlphaImager 3400 software (Alpha Innotech, San Leandro, CA). Background from a mock immunoprecipitation was subtracted. Values presented are the mean percentages relative to wild type (CY4353; *TRA1 TTI2*) of the ratio of acetylated histone (AcH3 or AcH4) to

total histone H3 for two independent experiments. *PGK1* promoter primers were 2927-1 and 2927-2.

Fluorescence microscopy

Yeast cells expressing eGFP and/or RFP fusions were grown in synthetic complete (SC) media, then diluted 1:4 into synthetic complete media with or without 8% ethanol. Growth in ethanol was for 18 hr. Prior to visualization, cells were concentrated 10-fold and 4′6-diamidino-2-phenylindole (DAPI) added to 0.02 mg/ml. Fluorescent images were obtained using a Zeiss Axioskop 2 microscope driven by ImageJ 1.41 software (National Institutes of Health) and a Scion CFW Monochrome CCD Firewire camera (Scion, Frederick MD) using DAPI, RFP, and GFP filter sets. Quantification of GFP signal intensity was performed using ImageJ software (version 1.45). The *freehand selections* tool was used to trace each whole cell and nucleus separately. The *measure* function output the signal intensity per unit area for each selection. To correct for background, the average intensity of three background selections adjacent to each cell was subtracted. The corrected nuclear intensity was then divided by the corrected whole cell intensity to give a nuclear-to-cell intensity ratio. The mean from 20 cells was calculated plus/minus a standard deviation.

Results

Isolation of suppressors of tra1-F3744A

We previously demonstrated that the extreme C terminus of Tra1, the FATC domain, plays a key role in the protein's function (Hoke *et al.* 2010). Altering the terminal Phe of Tra1 results in temperature sensitivity and slow growth in media containing 6% ethanol, Calcofluor white, or rapamycin. As shown in Figure 1A, growth of a strain containing the *tra1-F3744A* allele is impaired in a variety of other stress conditions including media depleted of phosphate and containing galactose as the carbon source. The allele does not result in sensitivity to all stress, as the strain was relatively resistant to high concentrations of sodium chloride or sorbitol. To address the role of this region of Tra1, we initiated a genetic screen to identify suppressors of the *tra1-F3744A* allele. We plated ∼2 million cells and subjected them to UV radiation at a dose that allowed 10% viability. Three colonies were isolated on the basis of their fast growth in YPD at
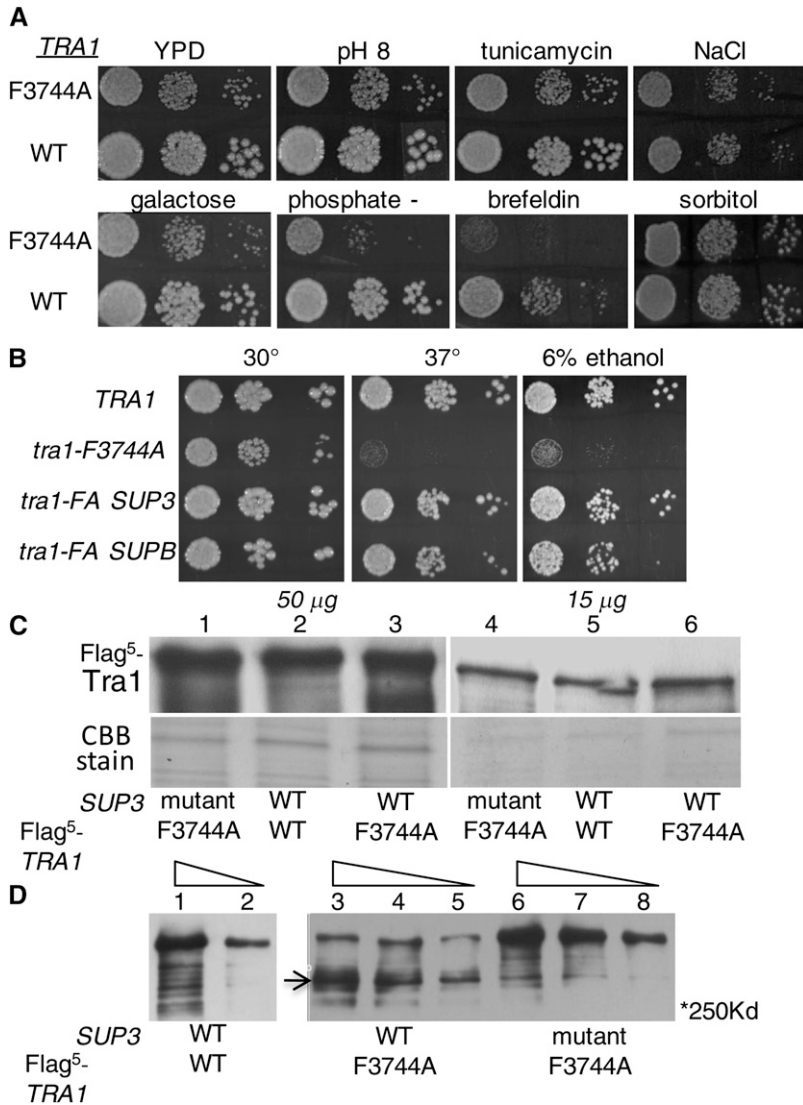
Figure 1 Isolation of extragenic suppressors of tra1-F3744A. (A) Phenotypes resulting from *tra1-F3744A*. Yeast strains CY4350 (*tra1-F3744A*) and CY4353 (*TRA1*) containing YCplac33-YHR100C (included since the *HIS3* allele used to select for *TRA1* integration disrupts the terminal 11 codons of YHR100C) were grown to stationary phase in media lacking uracil. Tenfold serial dilutions were spotted onto YP containing 2% glucose (YPD) or 2% galactose, or YPD with 1.0 μg/ml tunicamycin, 1.2 M NaCl, 60 μg/ml brefeldin, or 1.0 M sorbitol. YPD media was also depleted of phosphate (Han *et al.* 1988) or made to pH 8.0 with the addition of sodium hydroxide. Plates were grown at 30°. (B) Suppression of *tra1-F3774A* by alleles of *tti2*. Cultures of yeast strains CY4353 (*TRA1*), CY4350 (*tra1-F3744A*), CY5667 (*tra1-F3744A tti2*-F328S; *SUP3*), and CY5842 (*tra1-F3744A tti2-I336F*; *SUPB*) containing YCplac33-YHR100C were serially diluted and spotted onto a YPD plate or YPD containing 6% ethanol and grown at 30° or 37°. Note that *SUP3* and *SUPB* are *tti2-F328S* and *tti2-I336F*, respectively. (C) Yeast strains CY5912 (lanes 1 and 4; Flag[5]-*tra1-F3744A/tra1-F37443A tti2-F328S/tti2-F328S*; *SUP3* mutant), CY4419 (lanes 2 and 5; *Flag[5]-TRA1/TRA1 TTI2/TTI2*; *SUP3* WT), and CY4421 (lanes 3 and 6; *Flag[5]-tra1-F3744A/TRA1 TTI2/TTI2*; *SUP3* WT) were grown to stationary phase in minimal media depleted of uracil, then diluted 1/20 into YPD and grown for 8 hr at 30°. A total of 50 μg or 15 μg of protein extract prepared by grinding with glass beads was separated by SDS–PAGE (5%) and Western blotted with anti-Flag antibody (top) or stained with Coomassie Brilliant Blue (CBB stain, bottom). (D) Yeast strains CY6072 (lanes 1 and 2; Flag[5]-*TRA1 YCplac111-TTI2*), CY6074 (lanes 3–5; *Flag[5]-tra1-F3744A YCplac111-TTI2*), and CY6083 (lanes 6–8; *Flag[5]-tra1-F3744A YCplac111-tti2-F328S*) were grown in YPD to an optical density of 600 nm of ~2.0. Protein extracts were prepared by grinding in liquid nitrogen and clarified by centrifugation. Serial dilutions of each were separated by electrophoresis, and Flag[5]-tagged Tra1 or Tra1-F3744A was detected by Western blotting. The proteolytic product of ~300 kDa is indicated by an arrow.

37°. Each of these isolated strains also grew in media containing 6% ethanol. To determine whether the suppressor mutations were linked to *tra1-F3744A*, the suppressor strains were crossed with a strain containing *tra1-F3744A* positioned downstream of a *URA3* marker (CY5928). Analysis of the resulting tetrads revealed that each of the suppressors segregated as a single mutation, and one of the three (*SUP3*) was not closely linked to *tra1-F3744A*. A second independent screen was performed starting with ~10 million cells and selecting for growth at 35° on media containing 4% ethanol. Again one unlinked suppressor (*SUPB*) was obtained. Growth of a wild-type strain (CY4353), the *tra1-F3744A* strain (CY4350), and the two suppressor strains on YPD at 30° and 37°, and on YPD containing 6% ethanol is shown in Figure 1B.

We analyzed the expression of Tra1-F3744A in wild-type and *SUP3*-containing strain backgrounds to address whether the suppressor altered the expression of Tra1. Diploid strains with one copy of Flag[5]-Tra1 or Flag[5]-Tra1-F3744A were grown in YPD media. As shown in Figure 1C, the amount of Flag[5]-tagged Tra1-F3744A (lanes 3 and 6) is similar to wild-type Tra1 (lanes 2 and 5). This level is not altered by the *SUP3* mutation (lanes 1 and 4), indicating that suppression is not mediated through a change in Tra1 expression. The protein shown in Figure 1C was prepared by lysis with glass beads to minimize the processing time. We have seen changes in the profiles when extracts are prepared by grinding in liquid nitrogen and subjected to a further hour-long centrifugation. Figure 1D shows a representative profile for Flag[5]-tagged Tra1 or Tra1-F3744A in haploid strains grown in YPD media. We observe a pronounced proteolytic product of ~300 kDa for Flag[5]-Tra1-F3744A (arrow, lanes 3–5), which is minimal for wild-type Flag[5]-Tra1 (lanes 1 and 2), suggesting that the F3744A change may alter the conformation of Tra1. This proteolytic fragment was reduced in a strain containing a plasmid copy of *SUP3* (lanes 6–8).
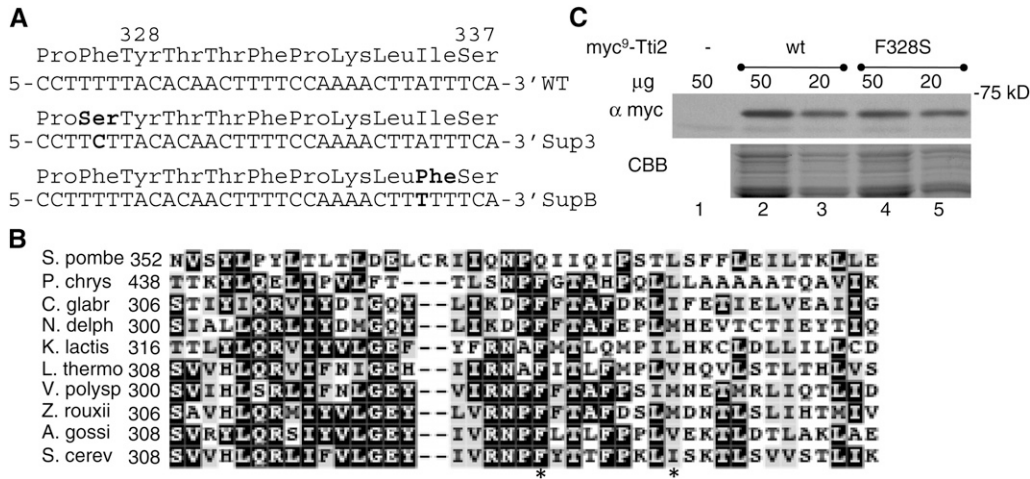
A

```
        328                                337
        ProPheTyrThrThrPheProLysLeuIleSer
5-CCTTTTTACACAACTTTTCCAAAACTTATTTCA-3' WT

        ProSerTyrThrThrPheProLysLeuIleSer
5-CCTTCTTACACAACTTTTCCAAAACTTATTTCA-3' Sup3

        ProPheTyrThrThrPheProLysLeuPheSer
5-CCTTTTTACACAACTTTTCCAAAACTTTTTTCA-3' SupB
```

C

myc^9-Tti2   -   wt   F328S
μg   50   50   20   50   20   -75 kD
α myc
CBB
1   2   3   4   5

B

```
S. pombe   352  MVSYLPYLTLTLDELCRILQNPQIIQIPSTLSFFLEILTKLLE
P. chrys   438  TTKYLQELIPVLFT----TLSNPFGTAHPQLLLAAAAATQAVIK
C. glabr   306  SILYLQRVIYDIGQY--LIKDPFFTAFDKLIFELIELVEAIIG
N. delph   300  SIALLQRLIYDMGQY--LIKDPFFTAFEPLMHEVTCTIEYTIQ
K. lactis  316  TTLYLQRVIIVLGEF--YFRNAFMLQMPILHKCLDLLILLCD
L. thermo  308  SVVHLQRVIFNIGEH--IIRNAFIALFMLVHQVLSTLTHLVS
V. polysp  300  SVIHLSRLIFNLGEY--VIRNPFFTAFSIMNELMRLIQTLID
Z. rouxii  306  SAVHLQRMIYVLGEY--LVRNPFTAFDSLMDNTLSLIHTMIV
A. gossi   308  SVRYLQRSIYVLGEY--IVRNPFLTLFPPLVEKTLDTLAKLAE
S. cerev   308  SVVHLQRLIFVLGEY--IVRNPFYATFPKLISKTLSVVSTLTK
                                  *              *
```

Figure 2 Alleles of TTi2 suppress tra1-F3744A. (A) Sequence of the suppressor *tti2* alleles. (B) Multiple sequence alignment of Tti2 from a variety of fungal species. The two alterations found in the suppressor strains are indicated by asterisks. The alignment was performed with MUSCLE (Edgar 2004). In order, the proteins are: *Schizosaccharomyces pombe*, NP_596623.3; *Penicillium chrysogenum*, XP_002568898.1; *Candida glabrata*, XP_449362.2; *Nakaseomyces delphensis*, CAO98781.1; *Kluyveromyces lactis*, XP_451713.1; *Lachancea thermotolerans*, XP_0025553740.1; *Vanderwaltozyma polyspora*, XP_001643571.1; *Zygosaccharomyces rouxii*, XP_002495325.1; *Ashbya gossypii*, NP_982872.1; *Saccharomyces cerevisiae*, NP_012670.1. (C) Yeast strain BY4743 containing YCplac111 (lane 1), YCplac111-myc^9-*TTI2* (lanes 2 and 3), or YCplac111-myc^9-*tti2-F328S* (lanes 4 and 5) were grown to stationary phase in minimal media depleted of leucine, then diluted 1/20 into YPD and grown for 8 hr at 30°. A total of 20 or 50 μg of protein from each was separated by SDS–PAGE (10%) and Western blotted with anti-myc antibody (top) or stained with Coomassie Brilliant Blue (CBB, bottom).

Identification of SUP3 and SUPB as alleles of TTI2

To identify the *SUP3* mutation, the suppressor-containing strain was backcrossed with the parent CY4350 (or CY4351) nine times, each time selecting for spore colonies that grew in ethanol and at 37°. After the ninth backcross, genomic DNA was isolated from three strains: an ethanol/37°-resistant spore colony and a sensitive spore colony from the same tetrad and an ethanol/37°-resistant spore colony from a distinct tetrad. Libraries were prepared and genomic sequencing was performed using the ABI SOLiD 4.0 platform at the Centre for Applied Genomics at The Hospital for Sick Children (Toronto, Ontario, Canada). The sequencing was performed in a single lane, multiplexing with 12 additional unrelated samples. Approximately 50 million reads were obtained for each sample, 60% of which aligned to the reference genome from the *Saccharomyces* Genome Database. Four single nucleotide differences were shared between the 37°/ethanol resistant strains and not found in the sensitive strain. Only one of these differences, a T- to-C change within codon 328 of *TTI2*, was found upon manual inspection of individual sequence reads. This T- to-C transition converts amino acid residue Phe328 to Ser (Figure 2A), a position highly conserved in the fungal Tti2 proteins (Figure 2B; a closely related region is not apparent in human Tti2, C8ORF41). As shown by the Western blot in Figure 2C, the F328S mutation did not alter expression of Tti2.

Two approaches were used to demonstrate that suppression of *tra1-F3744A* was the result of *tti2-F328S*. As shown in Figure 3A, *SUP3* is partially dominant, with suppression being slightly less in a heterozygous diploid as compared to a haploid strain. We compared this effect with the addition of wild-type *TTI2* to CY4350 (*tra1-F3744A*) on a centromeric plasmid (Figure 3B). As was found for the heterozygous diploid, addition of the *TTI2*-containing plasmid partially, but not completely, reversed the effect of *tti2-F328S*. Second, we analyzed eight independent spore colonies, six resistant and two sensitive, from a cross of CY5667 (*tti2-F328 tra1-F3744A*) and CY4350 (*TTI2 tra1-F3744A*). The *TTI2* allele from each spore colony was isolated by PCR and sequenced. For each of the eight alleles, *tti2-F328S* was found in all of the resistant strains and none of the sensitive strains. As the characteristics of the independently derived *SUPB* and *SUP3* strains were highly similar, having identified *tti2-F328S* as *SUP3*, we sequenced the *TTI2* allele in a derivative of the original *SUPB* strain that had been backcrossed *vs.* its parent seven times. One mutation was observed, an A-to-T at the first position of codon 336, converting isoleucine 336 to phenylalanine. The *TTI2* allele from four spore colonies was sequenced; the *tti2-I336F* mutation segregated 2:2 with the suppressor phenotype.

Tti2 is a component of the Tra1-containing ASTRA complex and associates with Tel1 and Tor1 in part of what may be a chaperone complex with Tel2 and Tti1 (Shevchenko *et al.* 2008; Hurov *et al.* 2010; Takai *et al.* 2010; Helmlinger *et al.* 2011). To better understand the interactions of the *tti2* mutations with *TRA1*, we examined the growth of single and double mutant strains under a variety of conditions (Figure 4; also see Figure S2). Both the *tti2-F328S* and *I336F* mutations suppressed the effects of *tra1-F3744A* under all of the conditions examined. Interestingly, this included reversal of the enhanced growth resulting from *tra1-F3744A* seen in media containing geneticin (G418), and the slow growth due to the DNA damaging agents MMS and phleomycin. Also of note the *tti2-F328S* allele in isolation resulted in minimal phenotypes; the *tti2-F328S* strain had a very slight reduction in growth in media depleted of phosphate.
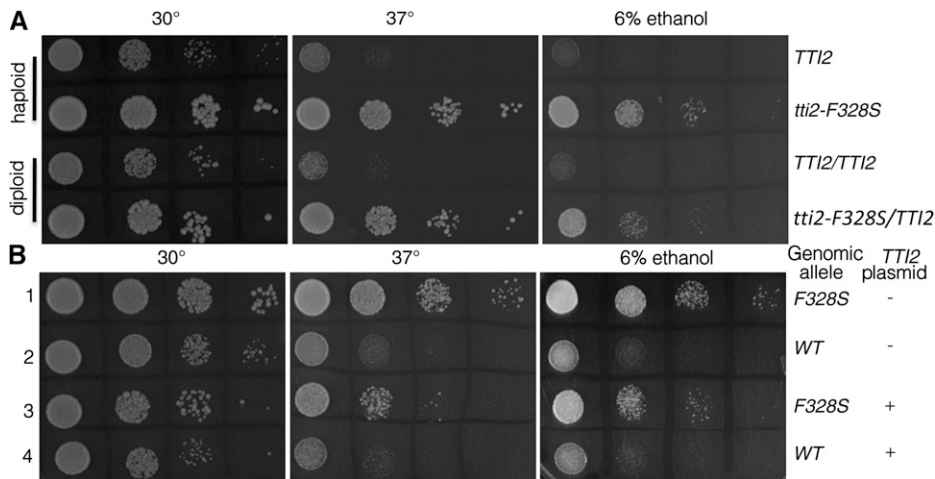
Figure 3 tti2-F328S acts as a partial dominant allele. (A) Genomic complementation. The haploid yeast strains CY4350 (tra1-F3744A TTI2) and CY5667 (tra1-F3744A TTI2-F328S) and diploid strains homozygous for tra1-F3744A and either homozygous or heterozygous for TTI2-F328S were grown to stationary phase and serial dilutions spotted onto YPD plates and grown at 30° or 37° or YPD containing 6% ethanol and grown at 30°. (B) Plasmid complementation. CY5667 (lanes 1 and 3) and CY4350 (lanes 2 and 4) were transformed with YCplac111-myc⁹-TTI2 or vector alone. Serial dilutions of the strains were spotted on the plates indicated.

tti2-F328S suppresses transcriptional defects due to tra1-F3744A

To determine whether the *tti2-F328S* allele restores the transcriptional competency of strains containing *tra1-F3744A*, we performed β-galactosidase assays with a *PHO5-lacZ* promoter fusion (Figure 5A). The *tra1-F3744A* allele decreases expression of *PHO5-lacZ* approximately fivefold as compared to wild-type *TRA1*. *tti2-F328S* suppressed this effect, resulting in expression that was 80% of wild type. *tti2-F328S* in the context of otherwise wild-type *TRA1* had only a marginal effect on *PHO5-lacZ* expression. *GAL10*, *HIS4*, and *RPL35a* lacZ-reporter fusions were also analyzed (Figure 5B). Similar to *PHO5*, *tra1-F3744A* decreased activated expression of *GAL10-lacZ* and expression of *HIS4-lacZ* approximately threefold. In both cases *tti2-F328S* restored expression to approximately wild-type levels. In contrast, the *RPL35a* promoter was relatively unaffected by *tra1-F3744A* or *tti2-F328S*.

We examined the effects of Tra1-F3744A on histone H4 acetylation (K8) as a ratio of the total histone H3 at the *PHO5* and *PGK1* promoters. Figure 6A shows the AcH4/H3 ratio for yeast strains CY4350 (tra1-F3744A TTI2) and CY5667 (tra1-F3744A tti2-F328S) as a percentage of that found for the wild-type strain CY4353 (TRA1 TTI2). Since histone H4 acetylation of *PHO5* is required prior to induction (Nourani *et al.* 2004), the chromatin immunoprecipitation was performed for cells grown in YPD media. The ratio of acetylated histone H4 to total histone H3 at *PHO5* was reduced to ~40% in the *tra1-F3744A* strain. In comparison, the ratio was ~90% of wild type at *PGK1*. The ~40% decrease for *PHO5* is somewhat less than the fourfold reduction seen upon deletion of the NuA4 component Eaf1 (Auger *et al.* 2008). Histone H4 acetylation returned to near wild-type levels in the presence of *tti2-F328S*. Figure 6B shows the analysis for acetylated histone H3 (K18) at *PHO5* for cells grown in low phosphate media (Nourani *et al.* 2004). In contrast to histone H4 acetylation, Tra1-F3744A had virtually no effect on histone H3 acetylation (AcH3/total H3). Under the same conditions, deletion of Ada2, a direct regulator of Gcn5, reduced histone H3 acetylation by ~20-fold.

Allele specificity of tti2-F328S

We examined the ability of *tti2-F328S* to suppress deletions within the genes of other components of the SAGA and NuA4 complexes. Similar to the effect of *tra1-F3744A*, deletions of *ada2* or *spt7* result in slow growth on media containing ethanol. However, unlike *tra1-F3744A*, slow growth caused by *ada2Δ* and *spt7Δ* was not suppressed by *tti2-F328S* (Figure 7A). Disruption of the gene encoding the NuA4 component Eaf3 results in slow growth in media containing Calcofluor white plus staurosporine (Figure 7B). Slow growth of an *eaf7* disruption is observed for cells grown in 6% ethanol at 35°. Neither of these phenotypes was suppressed by *tti2-F328S* (Figure 7B). As a strain with a disruption of *YNG2* was not available in an isogenic background, suppression by *tti2-F328S* was analyzed by taking advantage of its dominant nature. YCplac111-tti2-F328S was transformed into QY202 (*yng2Δ*; kindly supplied by Jacques Côtè) and QY202 (*YNG2*). As shown in Figure 7C, the plasmid copy of *tti2-F328S* did not suppress slow growth of the *yng2Δ* strain at 30°. We also analyzed the ability of *tti2-F328S* to suppress a second *tra1* FATC domain mutation, *tra1-L3733A*, as well as a triple alanine scanning mutation of residues 3413–3315 (*tra1-SRR₃₄₁₃*; Mutiu *et al.* 2007) within the PI3K domain. As shown in Figure 7D, *tti2-F328S* partially suppressed the temperature sensitivity and slow growth in ethanol seen for the *tra1-L3733A* strain, though not as efficiently as for *tra1-F3744A* (compare to Figure 7A). In contrast, *tti2-F328S* did not suppress the slow growth of the *tra1-SRR₃₄₁₃* strain at 37°, but rather augmented the slow growth phenotype (Figure 7E).

Localization of Tti2 and Tti2-F328S

We expressed N-terminally eGFP-tagged Tti2 and Tti2-F328S in BY4741 to determine whether the F328S mutation altered its localization (Figure 8). The wild-type molecule was found throughout the cell with both cytoplasmic and nuclear localization. When stressed with 6% ethanol, the distribution was relatively unchanged though some foci were observed. The proximity to the vacuole suggests that
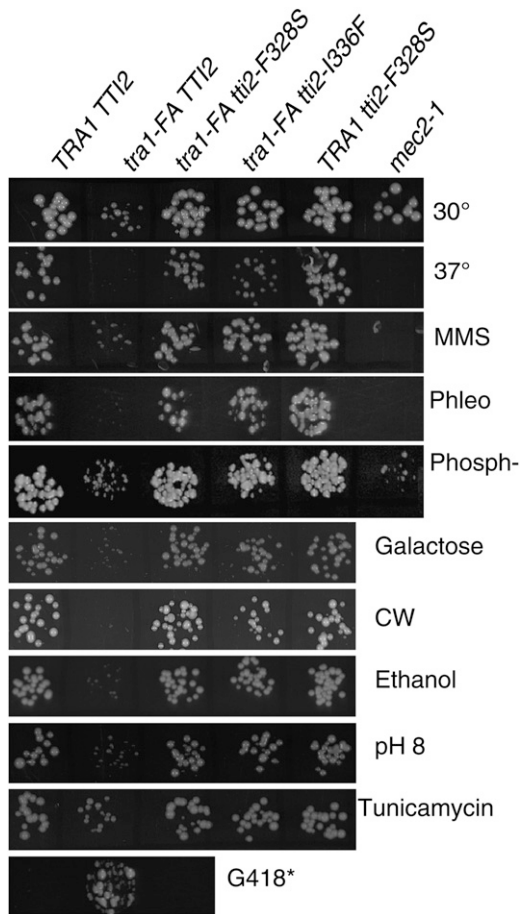
Figure 4 Suppression of tra1-F3744A phenotypes by tti2-F328S and tti2-I336F. Yeast strains CY4353 (TRA1 TTI2), CY4350 (tra1-F3744A TTI2), CY5667 (tra1-F3744A tti2-F328S), CY5843 (tra1-F3744A tti2-I336F), CY5665 (TRA1 tti2-F328S), or a mec2-1 strain (Weinert *et al.* 1994; included to verify the phleomycin and MMS plates) were grown to stationary phase diluted 1/10⁴ and spotted onto selection plates as follows: YPD at 30°, YPD at 37°; YPD at 30° containing 0.03% methyl methanesulfonate 0.03% (MMS), 1.0 μg/ml phleomycin (Phleo), YPD depleted of phosphate (Phosph−), 7.5 μg/ml Calcofluor White (CW), 6% ethanol, 1.0 μg/ml tunicamycin, or 20 μg/ml geneticin (G418); YP containing 2% galactose, and YPD at pH 8.0. *Note that the plating on G418 was performed with no dilution of the cells.

these may be late endosomes. The localization of eGFP-Tti2-F328S was almost identical to the wild-type protein. In media containing 6% ethanol there was a slight reduction in vacuolar proximal foci, but this was variable.

Localization of Tra1 and Tra1-F3744A

We engineered yeast strains containing N-terminally eGFP-tagged Tra1 and Tra1-F3744A to examine their localization (Figure 9A). To avoid complications of slow growth due to the *tra1-F3744A* allele, the analysis was performed in heterozygous diploid strains with an untagged wild-type copy of Tra1. When grown in synthetic complete media wild-type eGFP-Tra1 was almost exclusively in the nucleus. Tra1-F3744A was found in the nucleus, but punctate fluorescence was also apparent in the cytoplasm. The amount of the cyto-
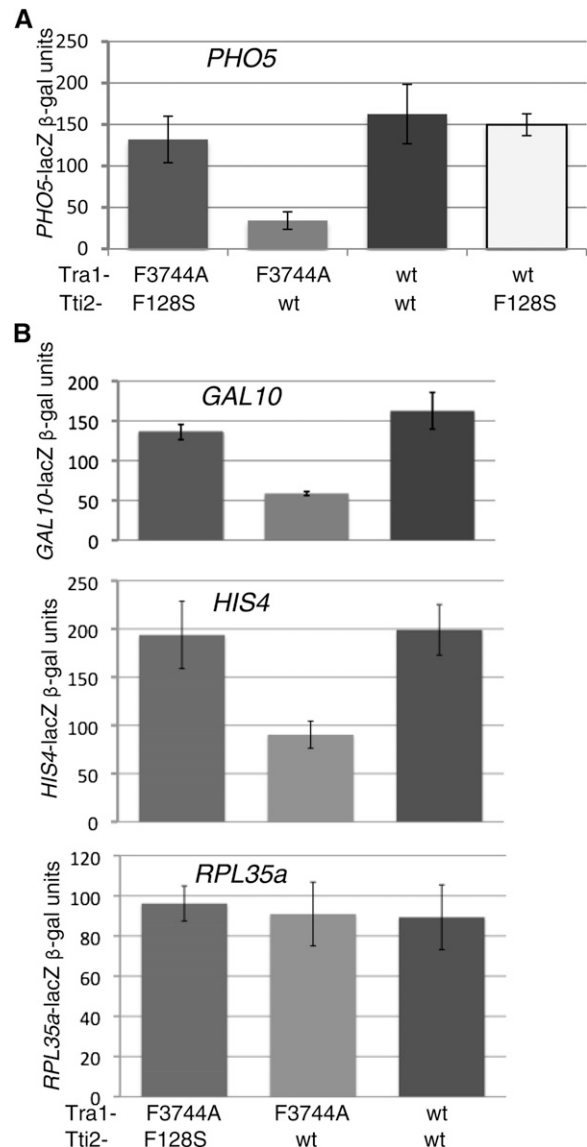

Figure 5 Expression of PHO5, GAL10, HIS4 and RPL35a promoter fusions in tti2-F328S strains. (A) Yeast strains CY5667, CY4350, CY4353, and CY5665 with the indicated *TRA1* and *TTI2* alleles, were transformed with a *LEU2* centromeric plasmid containing a *PHO5-lacZ* fusion, grown to stationary phase in media depleted of leucine, washed three times with water, diluted into YPD media depleted of phosphate, grown for 16 hr at 30°, and β-galactosidase activity was determined, normalizing to cell density. The error bars indicated represent one standard deviation from the mean. (B) *GAL10*, *HIS4*, and *RPL35a* promoters were analyzed as above in strains CY5667, CY4350, and CY4353. For *GAL10*, initial cultures were grown in raffinose containing media and shifted to 2% galactose. *HIS4* analysis was performed in media depleted of histidine. *RPL35a* was analyzed in YPD media.

plasmic eGFP-Tra1-F3744A was reduced in the heterozygous *tti2-F328S/TTI2* strain. In media containing 6% ethanol (Figure 9B), Tra1 was more disperse but the majority of the protein remained in foci, which we suggest are nuclear (DAPI staining was ineffective in this media). In ethanol-containing media, eGFP-Tra1-F3744A was diffusively distributed throughout the cytoplasm. Again, this appeared
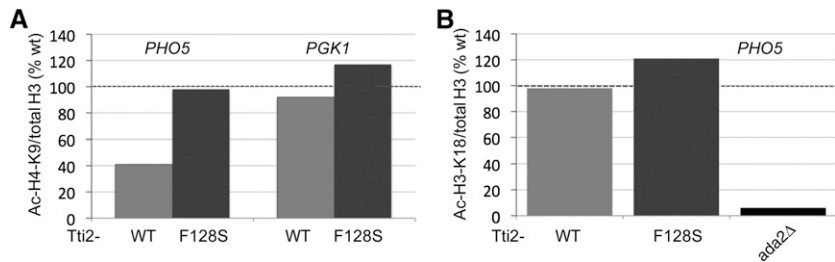
Figure 6 Histone H3 and H4 acetylation at the PHO5 promoter. (A) Histone H4 acetylation. Yeast strains CY4353 (*TRA1*), CY4350 (*tra1-F3744A*), and CY5667 (*tra1-F37744A tti2-F328S*) were grown to $A_{600} = 1.5$ in YPD media. ChIP analysis was performed using antibodies against acetylated K8 of histone H4 and against histone H3. Levels of immunoprecipitated *PHO5* and *PGK1* promoters were determined after PCR, separation of products by electrophoresis, and ethidium bromide staining. Serial dilutions were examined to ensure analysis in a linear range. The histogram shows the ratio of acetylated histone to total histone H3 (the mean for two independent experiments) for CY4350 and CY5667 as a percentage of the ratio found for the wild-type strain CY4353 (values for CY4353 are set at 100% and are not shown). (B) Histone H3 acetylation. Yeast strains CY4353 (*TRA1*), CY4350 (*tra1-F3744A*), CY5667 (*tra1-F37744A tti2-F328S*), and BY4282 (*ada2Δ*) were grown to $A_{600} = 1.5$ in YPD media depleted of phosphate. ChIP analysis was performed using antibodies against acetylated K18 of histone H3 and against histone H3. The histogram shows the average ratio of acetylated histone to total histone H3 for CY4350 and CY5667 as a percentage of the wild type (CY4353) for an experiment performed in duplicate.

partially reversed in the *tti2-F328S/TTI2* strain. We used imaging software to quantify the fluorescent intensity of GFP-Tra1 and GFP-Tra1-F3744A per unit area in the nucleus as compared to the whole cell (Table 3). For cells grown in ethanol, we assumed that the most pronounced focus was the nucleus. This quantification agrees with the visual conclusions drawn from the images of Figure 9 that Tra1-F3744A is more pronounced in the cytoplasm and partially relocalized to the nucleus by *tti2-F328S*.

To address the nature of the foci in which Tra1-F3744A is found, we visualized eGFG-Tra1-F3744A in strains containing RFP-tagged membrane constituents (Huh *et al.* 2003; strains kindly provided by Peter Arvidson). Figure 10A

shows the analysis with RFP-tagged Anp1 (Golgi apparatus), Sec13 (ER-to-Golgi vesicles), and Nic96 (nuclear periphery) in diploid strains (*eGFG-tra1-F3744A/TRA1*), when the cells were grown in media containing 6% ethanol. Of these, the closest overlap was seen with RFP-Anp1; however, precise colocalization with any one type of membrane was not evident, including additional analyses with Cop1, Pex3, and Snf7 (Figure S3). For comparison in Figure 10B, we show the localization of eGFP-Tra1-F3744A with the RFP-tagged proteins in synthetic complete media (no ethanol). As shown above, eGFP-Tra1-F3744A was more evident in the nucleus than in the presence of ethanol, but cytoplasmic eGFP-Tra1-F3744A was still apparent.
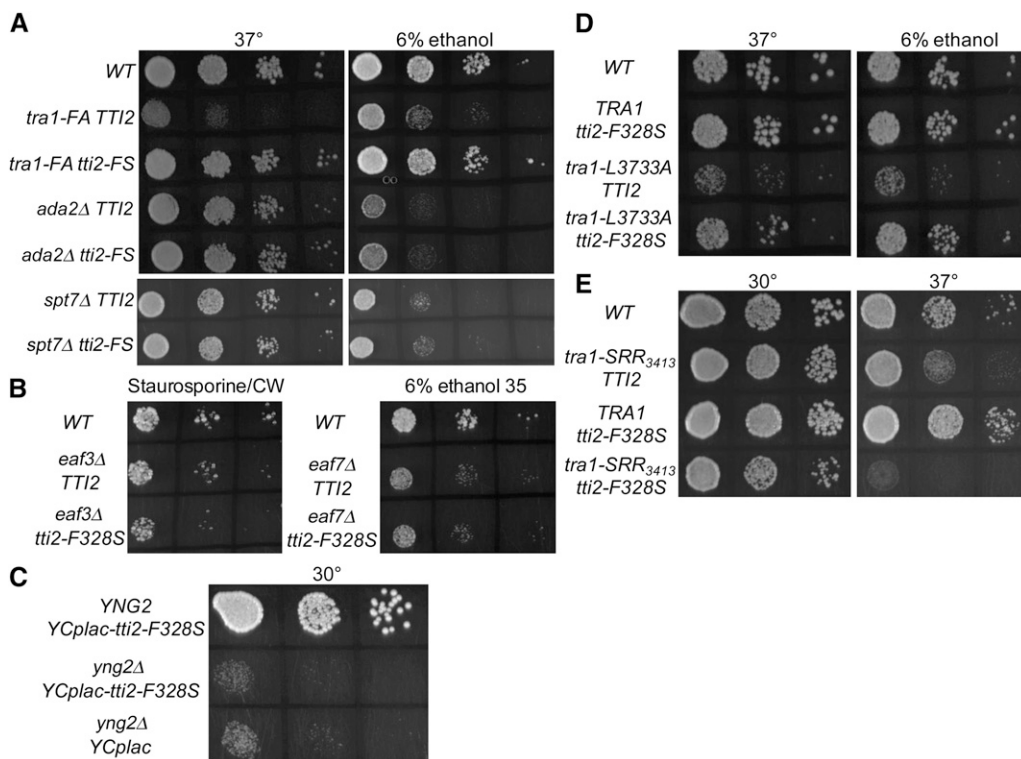

Figure 7 Allele specificity of tti2-F328S suppression. (A) SAGA components. Serial dilutions of yeast strains CY4353 (*TRA1 TTI2*), CY4350 (*tra1-F3744A TTI2*), CY5667 (*tra1-F37744A tti2-F328S*), BY4282 (*ada2Δ TTI2*), CY5876 (*ada2Δ tti2-F328S*), CY5873 (*spt7Δ TTI2*), and CY5915 (*spt7Δ tti2-F328S*) were spotted onto YPD (grown at 37°) or YPD with 6% ethanol (grown at 30°). The *spt7* deletion strains were grown on a separate plate and for an additional day. (B) NuA4 components. Yeast strains BY4742 (WT), BY7143 (*eaf3Δ TTI2*), CY5916 (*eaf3Δ tti2-F328S*), BY2940 (*eaf7Δ TTI2*), and CY5917 (*eaf7Δ tti2-F328S*) were spotted onto either YPD containing 1 μg/ml staurosporine plus 7.5 μg/ml Calcofluor White (grown at 30°) or 6% ethanol (grown at 35°). (C) yng2Δ. QY204 (*YNG2*) and QY202 (*yng2Δ0*) were transformed with *YCplac111-tti2-F328S* or *YCplac111*. Cultures were grown in media lacking leucine, and serial dilutions spotted onto YPD plates at 30°. (D) tra1-L3733A. Yeast strains CY4353, CY4350, CY4057 (*tral-L3733A TTI2*), and CY5658 (*tra1-L3733A tti2-F328S*) were spotted onto YPD at 37° and YPD containing 6% ethanol at 30°. (E) tra1-SRR$_{3413}$. Yeast strains CY4353, CY2222, (*tra1-SRR$_{3413}$ TTI2*), CY5665 (*TRA1 tti2-F328S*), and CY6137 (*tra1-SRR$_{3413}$ tti2-F328S*) were spotted onto YPD at 30° and 37°.
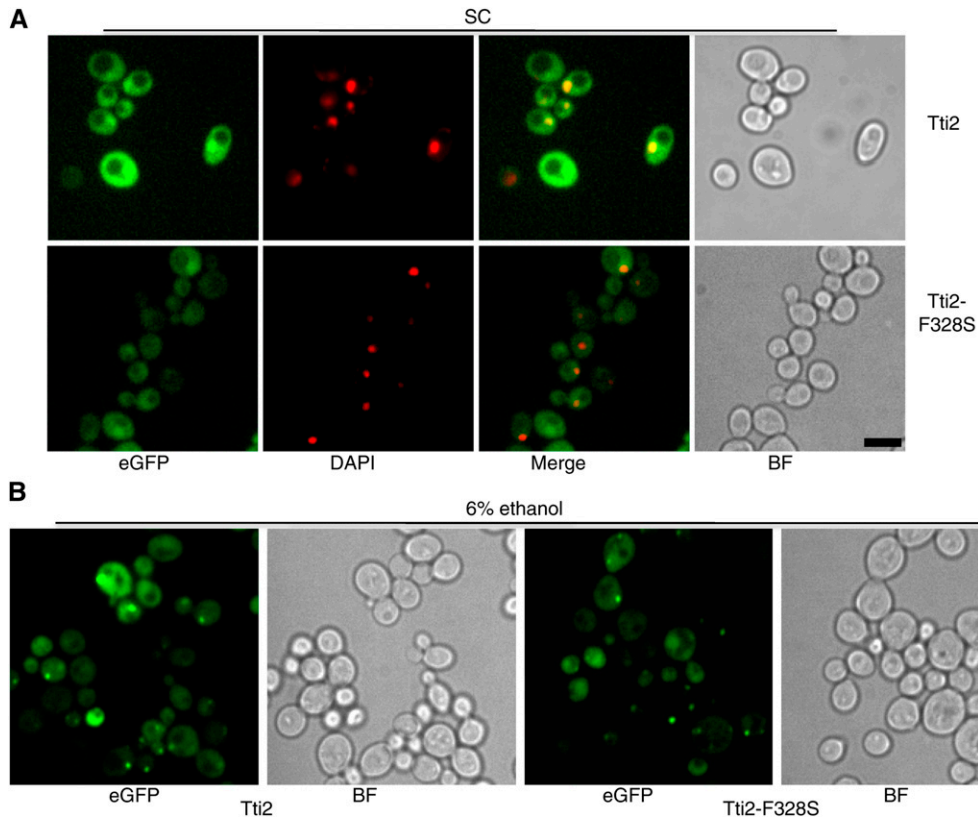
Figure 8 Localization of Tti2 and Tti2-F328S. (A) BY4741 containing *YCplac111-eGFP-TTI2* or *eGFP-tti2-F328S* were grown in synthetic complete (SC) media to late-log phase, stained with DAPI, and visualized by fluorescence microscopy. Bar, 10 μm (bottom right). (B) Above strains were grown to stationary phase in SC media, diluted 1:4 in SC media containing 8% ethanol, grown a further 18 hr, and visualized by fluorescence microscopy. BF, bright field.

If Tti2 has a role in the folding and/or stabilization of Tra1, strains with defects in the TTT complex may have reduced levels of Tra1. We introduced a *tel2-15* temperature-

sensitive allele (Stirling *et al.* 2011; Grandin *et al.* 2012) into a strain expressing Flag[5]-Tra1 and examined Tra1 levels after growth at 30°, 35°, and 37° (Figure 11A). The level of
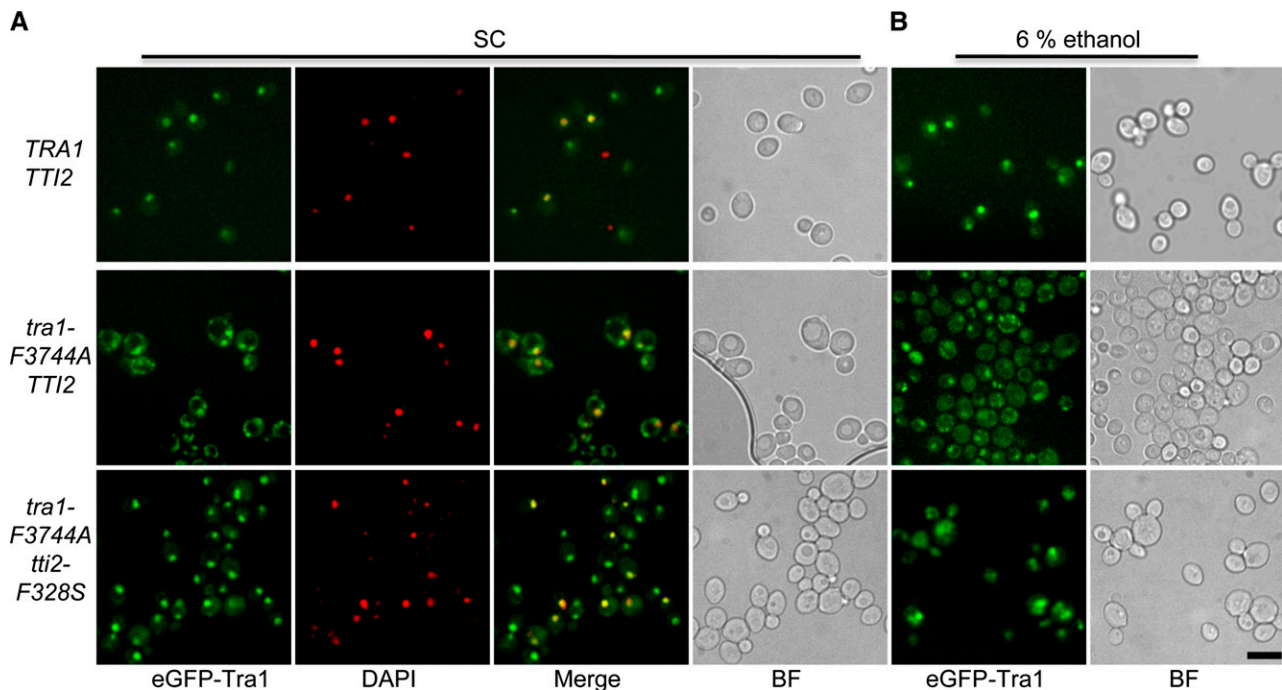

Figure 9 Localization of Tra1 and Tra1-F3744A. (A) Yeast strains CY6029 (*eGFP-TRA1/TRA1 TTI2/TTI2*), CY6025 (*eGFP-tra1-F3744A/TRA1 TTI2/TTI2*), and CY6063 (*eGFP-tra1-F3744A/TRA1 tti2-F328S/TTI2*) were grown in synthetic complete media to mid-log phase stained with DAPI and visualized by fluorescence microscopy (SC). (B) The two rightmost panels are strains grown in SC containing 6% ethanol. BF, bright field. Bar, 10 μm (bottom right).

Table 3 Relative concentrations (fluorescence intensity per unit area) of eGFP–Tra1 (wild type or F3744A) in the nucleus vs. total cell

	[Nuclear eGFP–Tra1]/[total cell eGFP–Tra1]	
Tra1/Tti2 (strain)	SC media	SC plus 6% ethanol
WT/WT (CY6029)	4.0 ± 0.6	2.4 ± 0.5
F3744A/WT (CY6025)	2.7 ± 0.5	2.0 ± 0.4
F3744A/F328S (CY6063)	3.5 ± 0.4	2.5 ± 0.5

Concentrations represent the intensity of eGFP fluorescence per unit area in the nucleus divided by the eGFP fluorescence per unit area for the cell (including the nucleus). Numbers represent the average for 20 cells. As DAPI staining was ineffective for the ethanol-grown cells, the most intense focus was assigned as the nucleus.

Flag[5]-Tra1 was unchanged by *tel2-15* at 30°, but substantially reduced at the two elevated temperatures. We also examined the phenotypes of strains containing *tel2-15*, a temperature-sensitive *tti2* allele (*tti2-1*, Stirling *et al.* 2011), or double mutations of these alleles in combination with *tra1-F3744A* (Figure 11B). The recessive *tel2-15* and *tti2-1*, alleles in an otherwise wild-type background, resulted in slow growth on media containing 6% ethanol at 30°. Under all of the conditions, *tel2-15* resulted in synthetic slow growth in combination with *tra1-F3744A*. A slight synthetic slow-growth phenotype was evident for the *tti2-1 tra1-F3744A* strain at 30°.

tra1-R3590I suppresses tra1-F3744A

Two recent analyses of PIKK structure suggest that the FATC domain may interact with and regulate the kinase domain (Lempiäinen and Halazonetis 2009; Sturgill and Hall 2009). To perhaps provide support for such a model, we sequenced the *tra1* allele 3′ of base 9730 in one of the intragenic suppressors of *tra1-F3744A*. A transversion of G-to-T at base 10,769, which converts arginine 3590 to isoleucine, was found. Alignments position R3590 in the putative activation loop, between β-sheet 10 and α-helix 7 corresponding to PI3K-γ (Figure 12A; Walker *et al.* 1999). To verify that R3590I is responsible for the suppression, the mutation was integrated into CY4398 and a haploid spore colony isolated after sporulation. The growth of this strain (CY5640; *tra1-R3590I-F3744A*) at 37°, and on media containing ethanol or rapamycin, confirmed that the R3590I mutation conferred suppression (Figure 12B). Similar to *tti2-F328S*, the F3590I mutation in isolation had no apparent phenotype.

Discussion

The FATC domain is essential for the function of Tra1 and other PIKK family members (Priestley *et al.* 1998; Beamish *et al.* 2000; Takahashi *et al.* 2000; Sun *et al.* 2005; Hoke *et al.* 2010). For Tra1, this is apparent from the fact that a protein containing an additional C-terminal glycine residue will not support viability (Hoke *et al.* 2010). Altering the terminal phenylalanine of Tra1 to alanine is less severe, but results in slow growth in rich media at 30° and under conditions of stress. We have shown that alleles of *TTI2* suppress *tra1-F3744A*. *tti2-F328S* restored all of the measured properties of the strains to ~80% of the wild-type level. Suppression by *tti2-F328S* was specific for mutations in the FATC domain of Tra1; *tra1-L3733A* was suppressed, whereas alleles altering the PI3K domain, or other SAGA or NuA4 components were not. The suppression by alleles of *TTI2*, whose product with Tel2 and Tti1 is proposed to act as a chaperone (Horejsí *et al.* 2010; Hurov *et al.* 2010; Kaizuka *et al.* 2010; Takai *et al.* 2010), the reduced levels of Tra1 in the *tel2-15* strain, and the increased number of proteolytic products seen after Western blotting Tra1-F3744A lead us to suggest that the FATC domain is important for Tra1 to acquire or stabilize a fully functional conformation. The finding that the F3744A mutation increased levels of cytoplasmic Tra1 is consistent with this model, or alternatively for roles of the FATC domain and Tti2 in protein trafficking. Loss of any of these possible roles would deplete functional Tra1 and would be expected to act broadly, given the importance of independent Tra1 (Helmlinger *et al.* 2011), as well as the SAGA and NuA4 complexes; indeed we find numerous phenotypic consequences of *tra1-F3744A*.

The eGFP-Tra1-F3744A present in the cytoplasm was not uniformly distributed, but appeared in foci. Though not specific for any one membrane type, we propose that these foci represent Tra1-F3744A associated with membranes and that the altered FATC domain potentially traps these molecules on the membranes. In turn, this finding predicts that the folding of Tra1 and perhaps the formation of some of its multisubunit complexes may occur on membranes. This is appealing because the membrane would provide a platform for the process to occur, and perhaps protect the C-terminal domains from proteolysis. A requirement for membrane interactions provides a rationale for the large number of synthetic interactions observed between membrane trafficking components and either *tra1-SRR₃₄₁₃* or deletions of NuA4 component genes (Hoke *et al.* 2008a; Mitchell *et al.* 2008). Membrane interactions are also consistent with the lipid binding properties of some of the SAGA components (Hoke *et al.* 2008b). In the event of reduced complex formation the molecules could be targeted to the vacuole, perhaps providing an explanation for the Pep4-dependent cleavage of Spt7 (Spedale *et al.* 2010). Interestingly, Han and Emr (2011) have recently shown that Cti6 and Tup1 assemble with Cyc8 on late endosomal membranes, mediated through their binding of phosphatidylinositol-3,5-diphosphate. Lipid binding is required for nuclear import of Cti6-Tup1-Cyc8, interaction with SAGA, and activation of galactose-regulated genes. Membranes are inherently sensitive to many environmental cues. As Han and Emr (2011) suggest, the membrane assembly of transcriptional complexes provides a tight link with the environmental state.

Our results in combination with the association of Tra1 and Tti2 determined by Shevchenko *et al.* (2008) clearly indicate a functional relationship between these molecules. The connection between Tel2, Tti2, and Tti1 demonstrated in mammalian cells suggests that the TTT complex is also functionally
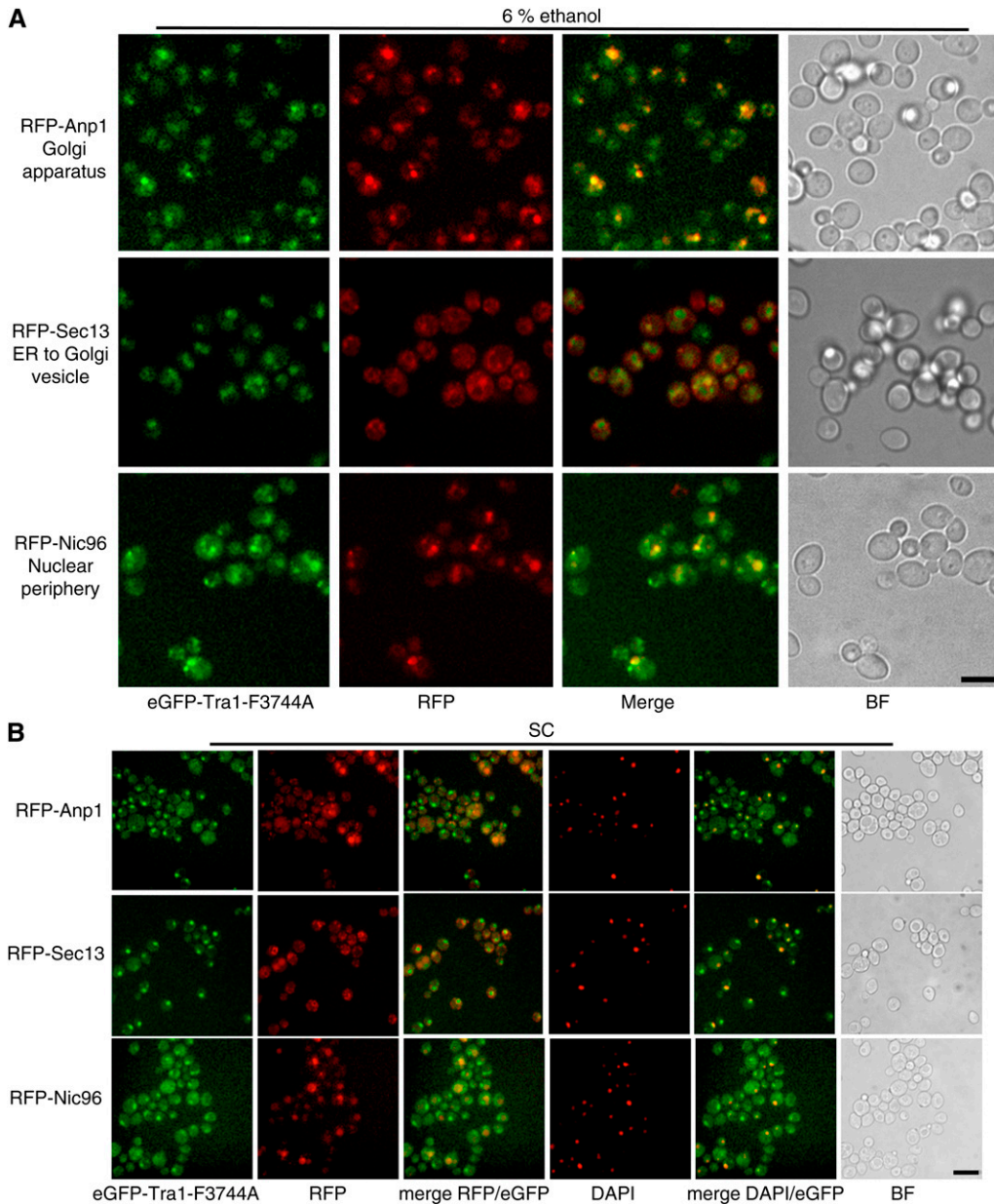
Figure 10 Localization of eGFP-Tra1-F3744A with RFP-tagged Anp1, Sec13, and Nic9. (A) Localization in SC media containing ethanol. Diploid strains containing a single copy of each tagged allele were grown to stationary phase in SC media, diluted 1:4 in SC containing 8% ethanol, grown a further 18 hr, and visualized by fluorescence microscopy. Bar, 10 μm (bottom right). (B) Localization in SC media. Columns 3 and 5 from the left are merged images between eGFP (green) and RFP or DAPI, respectively. Bar, 10 μm (bottom right).

associated with Tra1 (Hayashi *et al.* 2007; Takai *et al.* 2007, 2010; Hurov *et al.* 2010; Kaizuka *et al.* 2010). How this relates to other components of the ASTRA complex is less clear. In that it contains Rvb1 and Rvb2, ASTRA resembles an assembly of the R2TP (Huen *et al.* 2009 and TTT complexes with Tra1, similar to that seen for mTOR (Horejsí *et al.* 2010). The potential transient nature of ASTRA and its possible role in the folding/stability of Tra1 agrees with it not yet being isolated as an intact biochemical entity. Alternatively the suppression by Tti2 may take place in the context of an independent TTT complex, with ASTRA required for additional functions.

tti2-F328S acts in a partially dominant fashion to suppress *tra1-F3744A*. The suppression was most notable with *tti2-F328S* as the sole copy of the gene, but was still apparent in the context of the wild-type allele. With the specific mechanism of the TTT complex unknown, we can only speculate on how Tti2-F328S and Tti2-I336S act. A strict gain of function is possible, but perhaps less so given the two alleles and the partial dominance. Alternatively, the two mutations may disrupt an interaction or property of Tti2 that otherwise results in its inhibition. The dominant nature of the allele also suggested that the FATC domain of Tra1 might interact closely with the region of Tti2 surrounding F328. Tra1-F3744A may be unable to interact, and suppression result from the restored interaction with Tti2-F328S. The possibility of a direct interaction was attractive, given that a hydrophobic contact for the wild-type proteins could be replaced by a hydrogen bond between the serine of Tti2-F328S and the C terminus of Tra1. However, additional experiments were inconsistent with a direct contact. First this model would not easily explain suppression of *tra1-L3733A* or the ability of *tti2-I336F* to suppress. Second, if the domain of Tti2
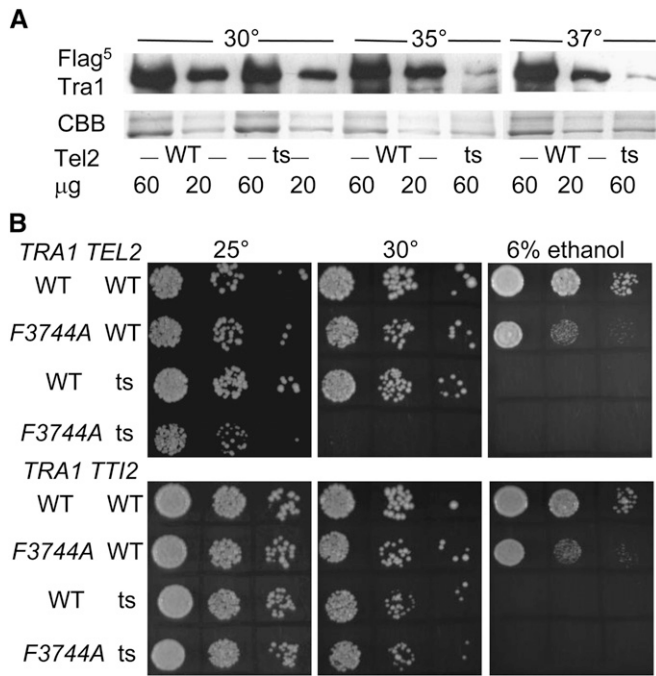
Figure 11 Interaction of tra1-F3744A with temperature sensitive alleles of components of the TTT complex. (A) Tel2 is required for the expression or stability of Tra1. Strains CY5919 (*Flag5-TRA1 TEL2, WT*) and CY6141 (*Flag⁵-TRA1 tel2-15*, *ts*) were grown to stationary phase at 30°, then diluted 20-fold into YPD and grown for 8 hr at 30°, 35°, or 37°. Whole cell extracts were prepared by bead lysis. The indicated amount of extract (60 or 20 μg) was separated by SDS–PAGE (5%). The upper half of the gel was Western blotted with anti-Flag antibody; the lower half was stained with Coomassie Brilliant Blue (CBB). (B) Growth of *tra1-F3744A* and *tel2-15* or *tti2-1* double mutant strains. CY4353 (wild-type), CY4350 (*tra1-F3744A*), PSY42 (*tel2-15*), PSY561 (*tti2-1*), CY6148 (*tra1-F3744A tel2-15*), and CY6146 (*tra1-F3744A tti2-1*) were grown to stationary phase at 25°, then serial dilutions plated onto YPD at 25° or 30° or YPD plus 6% ethanol at 30°.

were to directly contact the FATC domain, one might expect negative effects on the other FATC domain containing proteins. The only discernible phenotype of *tti2-F328S* in isolation was a slight slow growth in media depleted of phosphate. Tti2-F328S did not lead to sensitivity to the DNA damaging agents MMS or phleomycin, suggesting a minimal effect on Mec1 and Tel1. Finally, we were unable to detect an interac-

tion between a fragment of Tra1 containing the PI3K and FATC domains with the C-terminal half of Tti2 using recombinant proteins. We conclude that Tti2-F328S enhances the activity of Tra1-F3744A, likely by affecting folding, through a mechanism that does not restore interaction between the molecules or involve increased levels of Tti2. We note also that *tti2-F328S* does not suppress a mutation converting the terminal tryptophan of Mec1 to alanine (Figure S4). This suggests either that folding of the FATC domain of Mec1 does not require Tti2 function or that the change in function of Tti2-F328S is specific for Tra1.

Expression of the NuA4 (Nourani *et al.* 2004) and SAGA-regulated (Gregory *et al.* 1998) *PHO5* promoter was reduced approximately fivefold by *tra1-F3744A*. Consistent with an effect of this mutation on NuA4 function, Tra1-F3744A reduced histone H4 acetylation of the *PHO5* promoter. In contrast, and despite Gcn5 being required for activated expression, the F3744A mutation had little effect on histone H3 acetylation at the *PHO5* promoter. Since the breadth of the phenotypes attributable to *tra1-F3744A* suggests that SAGA function is altered, we propose that the lack of change in histone H3 acetylation is due to the ability of the Ada complex (Eberharter *et al.* 1999), including Gcn5, Ada2, and Ngg1, to act independently of SAGA. These results with Tra1-F3744A are similar to what we observe at *PHO5* upon deletion of Spt7: partially reduced acetylation, significantly decreased expression (D. Dobransky and C. J. Brandl, unpublished results). The lack of correlation between the importance of these molecules to *PHO5* expression and their effect on acetylation suggests that specific targeting of *PHO5* acetylation by SAGA is required for expression.

Our study is a direct demonstration of a functional link between Tra1 and Tti2. This link is likely the result of a role for Tti2, as part of the TTT complex, in the folding/maturation of Tra1 as has been found for other PIKK proteins (Takai *et al.* 2007, 2010; Horejsí *et al.* 2010; Hurov *et al.* 2010; Kaizuka *et al.* 2010; Stirling *et al.* 2011). In addition, our study points to a putative role for the FATC domain in the regulated folding/maturation of Tra1 in the cytoplasm. We cannot exclude that there are additional roles for the FATC domain. Recent models for the structure of the C-terminal domains of the PIKK family members predict that
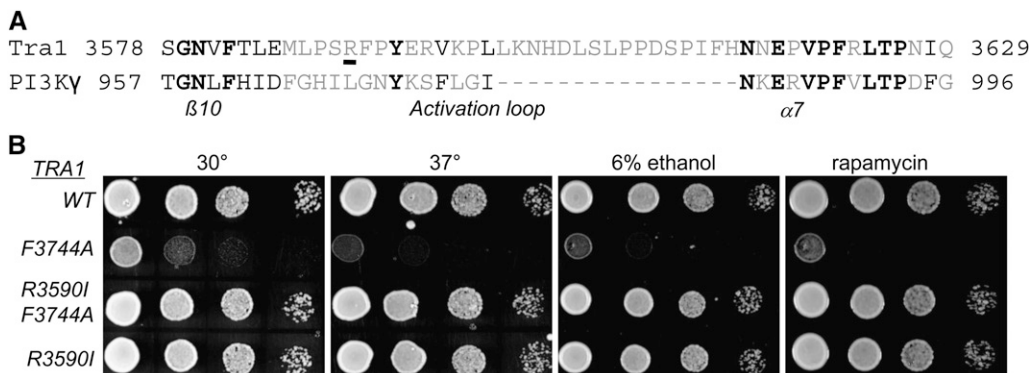

Figure 12 *tra1-R3590I* suppresses *tra1-F3744A*. (A) PI3K domain sequences of Tra1 (top) and porcine PI3K-γ (bottom) are aligned (SMART, Ponting *et al.* 1999) with structural features of porcine PI3K-γ (Walker *et al.* 1999) shown below. Arginine 3590 is underlined. (B) Cultures of yeast strains CY5920 (*TRA1*), CY5828 (*tra1-F3744A*), CY5640 (*tra1-R3590I, F3744A*), and CY5639 (*tra1-R3590I*) were serially diluted and spotted onto YPD (grown at 30° or 37°, 1 day) or YPD containing 6% ethanol or 1 nM rapamycin (2 days).

the helical FATC domain interacts and regulates the kinase domain (Lempiäinen and Halazonetis 2009; Sturgill and Hall 2009). The suppression of *tra1-F3744A* by mutation of arginine 3590 to isoleucine in the putative activation loop supports such an interaction. Interestingly, the models by Lempiäinen and Halazonetis (2009) and Sturgill and Hall (2009) place the C terminus in proximity to the active site where the FATC domain could have a role in catalysis.

Acknowledgments

Literature Cited

Abraham, R. T., 2004 PI 3-kinase related kinases: 'big' players in stress-induced signaling pathways. DNA Repair (Amst.) 3: 883–887.

Allard, S., R. T. Utley, J. Savard, A. Clarke, P. Grant et al., 1999 NuA4, an essential transcription adaptor/histone H4 acetyltransferase complex containing Esa1p and the ATM-related cofactor Tra1p. EMBO J. 18: 5108–5119.

Auger, A., L. Galarneau, M. Altaf, A. Nourani, Y. Doyon et al., 2008 Eaf1 is the platform for NuA4 molecular assembly that evolutionarily links chromatin acetylation to ATP-dependent exchange of histone H2A variants. Mol. Cell. Biol. 28: 2257–2270.

Ausubel, F. M., R. Brent, R. E. Kingston, D. D. Moore, J. G. Seidman et al., 1988 Current Protocols in Molecular Biology. Greene/Wiley-Interscience, New York, NY.

Beamish, H. J., R. Jessberger, E. Riballo, A. Priestley, T. Blunt et al., 2000 The C-terminal conserved domain of DNA-PKcs, missing in the SCID mouse, is required for kinase activity. Nucleic Acids Res. 28: 1506–1513.

Bhaumik, S. R., T. Raha, D. P. Aiello, and M. R. Green, 2004 In vivo target of a transcriptional activator revealed by fluorescence resonance energy transfer. Genes Dev. 18: 333–343.

Bosotti, R., A. Isacchi, and E. L. Sonnhammer, 2000 FAT: a novel domain in PIK-related kinases. Trends Biochem. Sci. 25: 225–227.

Brandl, C. J., A. M. Furlanetto, J. A. Martens, and K. S. Hamilton, 1993 Characterization of NGG1, a novel yeast gene required for glucose repression of GAL4p-regulated transcription. EMBO J. 12: 5255–5265.

Brown, C. E., L. Howe, K. Sousa, S. C. Alley, M. J. Carrozza et al., 2001 Recruitment of HAT complexes by direct activator interactions with the ATM-related Tra1 subunit. Science 292: 2333–2337.

Chittuluro, J. R., Y. Chaban, Y. J. Monnet-Saksouk, M. J. Carrozza, V. Sapountzi et al., 2011 Structure and nucleosome interaction of the yeast NuA4 and Piccolo NuA4 histone acetyltransferase complexes. Nat. Struct. Mol. Biol. 18: 1196–1203.

Dames, S. A., J. M. Mulet, K. Rathgeb-Szabo, M. N. Hall, and S. Grzesiek, 2005 The solution structure of the FATC domain of the protein kinase target of rapamycin suggests a role for redox-dependent structural and cellular stability. J. Biol. Chem. 280: 20558–20564.

Doyon, Y., and J. Côté, 2004 The highly conserved and multifunctional NuA4 HAT complex. Curr. Opin. Genet. Dev. 14: 147–154.

Dudley, A. M., C. Rougeulle, and F. Winston, 1999 The Spt components of SAGA facilitate TBP binding to a promoter at a post-activator step in vivo. Genes Dev. 13: 2940–2945.

Eberharter, A., D. E. Sterner, and D. Schieltz, A. Hassan, J. R. Yates III et al., 1999 The ADA complex is a distinct histone acetyltransferase complex in Saccharomyces cerevisiae. Mol. Cell. Biol. 19: 6621–6631.

Edgar, R. C., 2004 MUSCLE: multiple sequence alignment with high accuracy and high throughput. Nucleic Acids Res. 32: 1792–1797.

Fishburn, J., N. Mohibullah, and S. Hahn, 2005 Function of a eukaryotic transcription activator during the transcription cycle. Mol. Cell 18: 369–378.

Gansheroff, L. J., C. Dollard, P. Tan, and F. Winston, 1995 The Saccharomyces cerevisiae SPT7 gene encodes a very acidic protein important for transcription in vivo. Genetics 139: 523–536.

Grandin, N., L. Corset, and M. Charbonneau, 2012 Genetic and physical interactions between Tel2 and the Med15 Mediator subunit in Saccharomyces cerevisiae. PLoS ONE 7: e30451.

Grant, P. A., D. Schieltz, M. Pray-Grant, J. R. Yates III. and J. L. Workman, 1998 The ATM-related cofactor Tra1 is a component of the purified SAGA complex. Mol. Cell 2: 863–867.

Gregory, P. D., A. Schmid, M. Zavari, L. Lui, S. L. Berger et al., 1998 Absence of Gcn5 HAT activity defines a novel state in the opening of chromatin at the PHO5 promoter in yeast. Mol. Cell 1: 495–505.

Han, B.-K., and S. D. Emr, 2011 Phosphoinositide[PI(3,5)P$_2$] lipid-dependent regulation of the general transcriptional regulator Tup1. Genes Dev. 25: 984–995.

Han, M., U. J. Kim, P. Kayne, and M. Grunstein, 1988 Depletion of histone H4 and nucleosomes activates the PHO5 gene in Saccharomyces cerevisiae. EMBO J. 7: 2221–2228.

Hayashi, T., M. Hatanaka, K. Nagao, Y. Nakaseko, J. Kanoh et al., 2007 Rapamycin sensitivity of the Schizosaccharomyces pombe tor2 mutant and organization of two highly phosphorylated TOR complexes by specific and common subunits. Genes Cells 12: 1357–1370.

Helmlinger, D., S. Marguerat, J. Villen, D. L. Swaney, S. P. Gygi et al., 2011 Tra1 has specific regulatory roles, rather than global functions, within the SAGA co-activator complex. EMBO J. 30: 2843–2852.

Henry, K. W., A. Wyce, W. S. Lo, L. J. Duggan, N. C. Emre et al., 2003 Transcriptional activation via sequential histone H2B ubiquitylation and de ubiquitylation, mediated by SAGA associated Ubp8. Genes Dev. 17: 2648–2663.

Hoke, S. M. T., J. Guzzo, B. Andrews, and C. J. Brandl, 2008a Systematic genetic array analysis links the Saccharomyces cerevisiae SAGA/SLIK and NuA4 component Tra1 to multiple cellular processes. BMC Genet. 9: 46.

Hoke, S. M. T., J. Genereaux, G. Liang, and C. J. Brandl, 2008b A conserved region of yeast Ada2 regulates the histone acetyltransferase activity of Gcn5 and interacts with phospholipids. J. Mol. Biol. 384: 742–755.

Hoke, S. M., I.-A. Mutiu, J. Genereaux, S. Kvas, and M. Buck et al., 2010 Mutational analysis of the C-terminal FATC domain of Saccharomyces cerevisiae Tra1. Curr. Genet. 56: 447–465.

Horejsí, Z., H. Takai, C. A. Adelman, S. J. Collis, H. Flynn et al., 2010 CK2 phospho-dependent binding of R2TP complex to TEL2 is essential for mTOR and SMG1 stability. Mol. Cell 39: 839–850.

Huen, J., Y. Kakihara, F. Ugwu, K. L. Cheung, J. Ortega et al., 2010 Rvb1-Rvb2: essential ATP-dependent helicases for critical complexes. Biochem. Cell Biol. 88: 29–40.

Huh, W.-K., J. V. Falvo, L. C. Gerke, A. S. Carroll, R. W. Howson et al., 2003   Global analysis of protein localization in budding yeast. Nature 425: 686–691.

Hurov, K. E., C. Cotta-Ramusino, and S. J. Elledge, 2010   A genetic screen identifies the Triple T complex required for DNA damage signaling and ATM and ATR stability. Genes Dev. 24: 1939–1950.

Jha, S., and A. Dutta, 2009   RVB1/RVB2: running rings around molecular biology. Mol. Cell 12: 521–533.

Jiang, X., Y. Sun, S. Chen, K. Roy, and B. D. Price, 2006   The FATC domains of PIKK proteins are functionally equivalent and participate in the Tip60-dependent activation of DNA-PKcs and ATM. J. Biol. Chem. 281: 15741–15746.

Kaizuka, T., T. Hara, N. Oshiro, U. Kikkawa, K. Yonezawa et al., 2010   Tti1 and Tel2 are critical factors in mammalian target of rapamycin complex assembly. J. Biol. Chem. 285: 20109–20116.

Knutson, B. A., and S. Hahn, 2011   Domains of Tra1 important for activator recruitment and transcription coactivator functions of SAGA and NuA4 complexes. Mol. Cell. Biol. 31: 818–831.

Koutelou, E., C. L. Hirsch, and S. Y. Dent, 2010   Multiple faces of the SAGA complex. Curr. Opin. Cell Biol. 22: 374–382.

Langmead, B., C. Trapnell, M. Pop, and S. L. Salzberg, 2009   Ultrafast and memory-efficient alignment of short DNA sequences to the human genome. Genome Biol. 10: R25.

Lempiäinen, H., and T. D. Halazonetis, 2009   Emerging common themes in regulation of PIKKs and PI3Ks. EMBO J. 28: 3067–3073.

Li, H., B. Handsaker, A. Wysoker, T. Fennell, J. Ruan et al., 2009   The sequence alignment/map (SAM) format and SAMtools. Bioinformatics 25: 2078–2079.

Lovejoy, C. A., and D. Cortez, 2009   Common mechanisms of PIKK regulation. DNA Repair (Amst.) 8: 1004–1008.

Lustig, A. J., and T. D. Petes, 1986   Identification of yeast mutants with altered telomere structure. Proc. Natl. Acad. Sci. USA 83: 1398–1402.

McMahon, S. B., H. A. Van Buskirk, K. A. Dugan, T. D. Copeland, and M. D. Cole, 1998   The novel ATM-related protein TRRAP is an essential cofactor for the c-Myc and E2F oncoproteins. Cell 94: 363–374.

Mitchell, L., J. P. Lambert, M. Gerdes, A. S. Al-Madhoun, I. S. Skerjanc et al., 2008   Functional dissection of the NuA4 histone acetyltransferase reveals its role as a genetic hub and that Eaf1 is essential for complex integrity. Mol. Cell. Biol. 28: 2244–2256.

Mohibullah, S., and S. Hahn, 2008   Site-specific cross-linking of TBP in vitro and in vivo reveals a direct functional interaction with the SAGA subunit Spt3. Genes Dev. 22: 2994–3006.

Morita, T., A. Yamashita, I. Kashima, K. Ogata, S. Ishiura et al., 2007   Distant N- and C-terminal domains are required for intrinsic kinase activity of SMG-1, a critical component of nonsense-mediated mRNA decay. J. Biol. Chem. 282: 7799–7808.

Mutiu, A.-I., S. M. T. Hoke, J. Genereaux, C. Hannam, K. MacKenzie et al., 2007   Structure/function analysis of the phosphatidylinositol-3-kinase domain of yeast Tra1. Genetics 177: 151–166.

Nakada, D., Y. Hirano, Y. Tanaka, and K. Sugimoto, 2005   Role of the C terminus of Mec1 checkpoint kinase in its localization to sites of DNA damage. Mol. Biol. Cell 16: 5227–5235.

Nourani, A., Y. Doyon, R. T. Utley, S. Allard, W. S. Lane et al., 2001   Role of an ING1 growth regulator in transcriptional activation and targeted hstone acetylation by the NuA4 complex. Mol. Cell. Biol. 21: 7629–7640.

Nourani, A. R., R. T. Utley, S. Allard, and J. Côté, 2004   Recruitment of the NuA4 complex poises the PHO5 promoter for chromatin remodeling and activation. EMBO J. 23: 2597–2607.

Perry, J., and N. Kleckner, 2003   The ATRs, ATMs, and TORs are giant HEAT repeat proteins. Cell 112: 151–155.

Ponting, C. P., J. Schultz, F. Milpetz, and P. Bork, 1999   SMART: identification and annotation of domains from signalling and extracellular protein sequences. Nucleic Acids Res. 27: 229–232.

Priestley, A., H. J. Beamish, D. Gell, A. G. Amatucci, M. C. Muhlmann-Diaz et al., 1998   Molecular and biochemical characterisation of DNA-dependent protein kinase-defective rodent mutant irs-20. Nucleic Acids Res. 26: 1965–1973.

Reeves, W. M., and S. Hahn, 2005   Targets of the Gal4 transcription activator in functional transcription complexes. Mol. Cell. Biol. 25: 9092–9102.

Rodriguez-Navarro, S., 2009   Insights into SAGA function during gene expression. EMBO Rep. 10: 843–850.

Roth, S. Y., J. M. Denu, and C. D. Allis, 2001   Histone acetyltransferases. Annu. Rev. Biochem. 70: 81–120.

Saleh, A., D. Schieltz, N. Ting, S. B. McMahon, D. W. Litchfield et al., 1998   Tra1p is a component of the yeast Ada.Spt transcriptional regulatory complexes. J. Biol. Chem. 273: 26559–26565.

Shevchenko, A., A. Roguev, D. Schaft, L. Buchanan, B. Habermann et al., 2008   Chromatin Central: towards the comparative proteome by accurate mapping of the yeast proteomic environment. Genome Biol. 9: R167.

Sibandi, B. L., D. Y. Chirgadze, and T. L. Blundell, 2010   Crystal structure of DNA-PKcs reveals a large open-ring cradle comprised of HEAT repeats. Nature 463: 118–121.

Spedale, G., N. Mischerikow, A. J. Heck, H. T. Timmers, and W. W. Pijnappel, 2010   Identification of Pep4p as the protease responsible for formation of the SAGA-related SLIK protein complex. J. Biol. Chem. 285: 22793–22799.

Sterner, D. E., P. A. Grant, S. M. Roberts, L. J. Duggan, R. Belotesrkovskaya et al., 1999   Functional organization of the yeast SAGA complex: distinct components involved in structural integrity, nucleosome acetylation, and TATA-binding protein interaction. Mol. Cell. Biol. 19: 86–98.

Stirling, P. C., M. S. Bloom, T. Solanki-Patil, S. Smith, P. Sipahimalani et al., 2011   The complete spectrum of yeast chromosome instability genes identifies candidate CIN cancer genes and functional roles for the ASTRA complex components. PLoS Genet. 7: e1002057.

Sturgill, T. W., and M. N. Hall, 2009   Activating mutations in TOR are in similar structures as oncogenic mutations in PI3KCα. ACS Chem. Biol. 4: 999–1015.

Sun, Y., X. Jiang, S. Chen, N. Fernandes, and B. D. Price, 2005   A role for the Tip60 histone acetyltransferase in the acetylation and activation of ATM. Proc. Natl. Acad. Sci. USA 102: 13182–13187.

Sun, Y., X. Jiang, S. Chen, K. Roy, and B. D. Price, 2010   Tip60: connecting chromatin to DNA damage signaling. Cell Cycle 9: 930–936.

Takahashi, T., K. Hara, H. Inoue, Y. Kawa, C. Tokunaga et al., 2000   Carboxyl-terminal region conserved among phosphoinositide-kinase-related kinases is indispensable for mTOR function in vivo and in vitro. Genes Cells 5: 765–775.

Takai, H., R. C. Wang, K. K. Takai, H. Yang, and T. de Lange, 2007   Tel2 regulates the stability of PI3K-related protein kinases. Cell 131: 1248–1259.

Takai, H., Y. Xie, T. de Lange, and N. P. Pavletich, 2010   Tel2 structure and function in the Hsp90-dependent maturation of mTOR and ATR complexes. Genes Dev. 24: 2019–2030.

Walker, E. H., O. Perisoc, C. Ried, L. Stephens, and R. L. Williams, 1999   Structural insights into phosphoinositide 3-kinase catalysis and signaling. Nature 402: 313–320.

Weinert, T. A., G. L. Kiser, and L. H. Hartwell, 1994   Mitotic checkpoint genes in budding yeast and the dependence of mitosis on DNA replication and repair. Genes Dev. 8: 652–665.

Winzeler, E. A., and R. W. Davis, 1997   Functional analysis of the yeast genome. Curr. Opin. Genet. Dev. 7: 771–776.

Wu, P. Y., C. Ruhlmann, F. Winston, and P. Schultz, 2004   Molecular architecture of the S. cerevisiae SAGA complex. Mol. Cell 15: 199–208.

Communicating editor: K. Arndt

GENETICS

Genetic Evidence Links the ASTRA Protein Chaperone Component Tti2 to the SAGA Transcription Factor Tra1

Julie Genereaux, Stephanie Kvas, Dominik Dobransky, Jim Karagiannis, Gregory B. Gloor, and Christopher J. Brandl

```
                                               SphI
                                               GCATGC
TTTTAGCCGCCACTAATCAACTCCTTCAGATAGATCGCCAGAACGCAAA
TAAGTGAAATTTGAAGATCAACTTGAATCAAAAAGCCAAAACTAAGAATT
GTACGCTACTCTGCCAGACAATATTTTACGGACACGCGCATTTCAAGACA
AAGCCATAATTCATGCCTTTTCAACTAGCATCTGGACGCCGCTGAGATCA
HindIII
AAGCTTTAGGAACAAACAAAACGCACGAAAATAGCTAACGCACGTATCGA
ATACCAAATCAGTCTGCATTTATTGTACCCTCAAATTACAAATTCAACCA
ACAATTGTTCAAAAGACCACCTTGAATCTTGTGTTTCCTAATTTGGTAAG
TGATCACGTGGTCAGACAGTTTTCCAGGTCAAACTGAAAAAAAAGCTCAA
GAACCATTTTTCTTTAATAGCCTTTTTTAGTTGTATTCTAATAAACAACA
CCAACAAAATCGGAGGTATCACACGTAATTACATAAAGAAGATTAAATTC
AGAGAAGATCTATCACACGATATCTCCATAGTTACAAAGAATACCGCATT
            BamHI
TACAAAATGTCAGGATCCGATTATAAGGATCATGATGGTGACTACAAAGAC
CATGATATTGATTACAAGGATCATGACGGTGACTATAAAGATCATGATATT
                              NotI     SalI
GATTATAAAGATGATGACGATAAGGCGGCC  GCGTCGAC
```

Figure S1 Sequence of the molecule to integrate Flag[5]-tag TRA1. The ATG translational start preceding the tag is in bold. A genomic *Hind*III fragment encoding *URA3* (~1.1 kbp) was inserted at the underlined *Hind*III site. TRA1 sequences in frame with the *Not*I site (Saleh et al., 1998) were cloned 3' to the *Not*I.
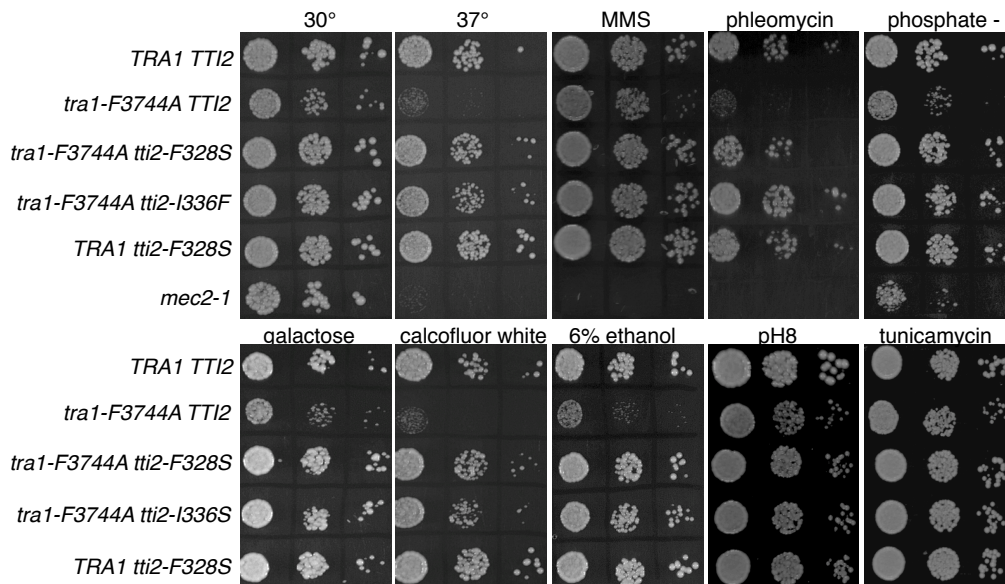
Figure S2 *Suppression of tra1-F3744A phenotypes by tti2-F328S and tti2-I336F*. Yeast strains CY4353 (*TRA1 TTI2*), CY4350 (*tra1-F3744A TTI2*), CY5667 (*tra1-F3744A tti2-F328S*), CY5843 (*tra1-F3744A tti2-I336F*), CY5665 (*TRA1 tti2-F328S*), or a *mec2-1* strain (Weinert *et al.*, 1994) were grown to stationary phase diluted 1/10[4] and serial dilutions spotted onto selection plates as follows: YPD at 30°, YPD at 37°; YPD at 30° containing 0.03% methyl methanesulfonate 0.03% (MMS), 1.0 μg/mL phleomycin, YPD depleted of phosphate, 7.5 μg/mL Calcofluor white, 6% ethanol, or 1.0 μg/mL tunicamycin; YP containing 2% galactose, and YPD at pH 8.0. Note that some images are composites from two otherwise identical plates.
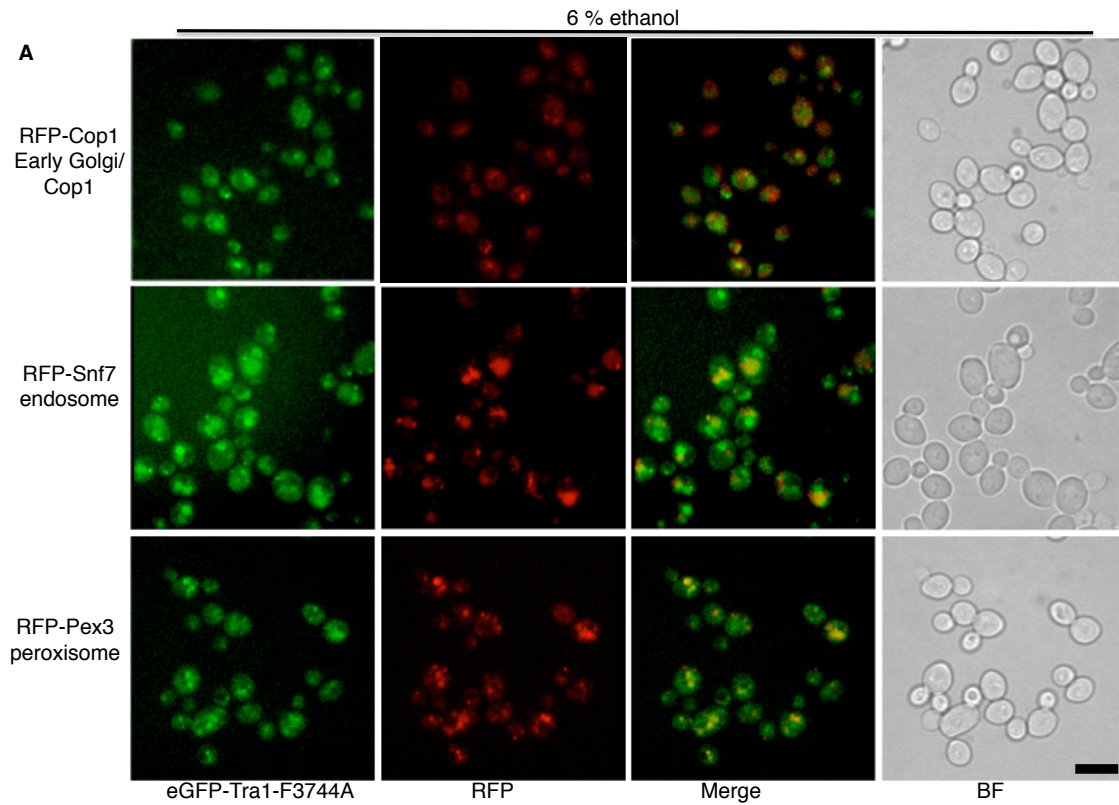
Figure S3 *Localization of eGFP-Tra1-F3744A with RFP-tagged Cop1, Snf7 and pex3 in SC media containing ethanol.* Diploid strains containing a single copy of each tagged allele were grown to stationary phase in SC media, diluted 1:4 in SC containing 8% ethanol, grown a further 18 hr, and visualized by fluorescence microscopy. A 10 µm scale bar is shown in the bottom right.

A

```
                                                   GCATGC GTTGATG
AATGTGATCG AAACAATTAT GTACGATAGA AACATGGACC ACTCAATTCA
AAAAGCGCTA AAGGTCTTAA GAAACAAAAT CCGCGGTATA GATCCGCAGG
ATGGCCTGGT ATTGAGTGTT GCTGGCCAAA CAGAAACATT GATCCAAGAA
GCAACATCAG AAGACAATCT AAGCAAGATG TATATTGGTT GGCTTCCATT
TGCTTGATCA CTTTCCACCA TTTTCGGCAA CAGACGAACT TCCTCTTGAT
CTAACCATCA CTGCAGGTGC TTTTCTCCGG CGGAGTTAAT GGATCCTTAT
CCCCGCTTCA TGTCATACTA TCTCTCTTAA CAGGGATGTT GACACCATAT
AAGTTAACAT AACATATACG TACGTAATAA TATTAAGGAC TATCTCGCAT
TTCAAAAGAG AAACAACCTA ATCAAGCCTT ATTATAAGAG CAAATTATTC
AAAAAAAGTC TACGGAGAAA ATTATTATGG TGGTTTTAGA CAAGAAGTTA
TTGGAAAGAT TGACTTCTCG TAAGGTTCCC TTAGAAGAGC TC
```
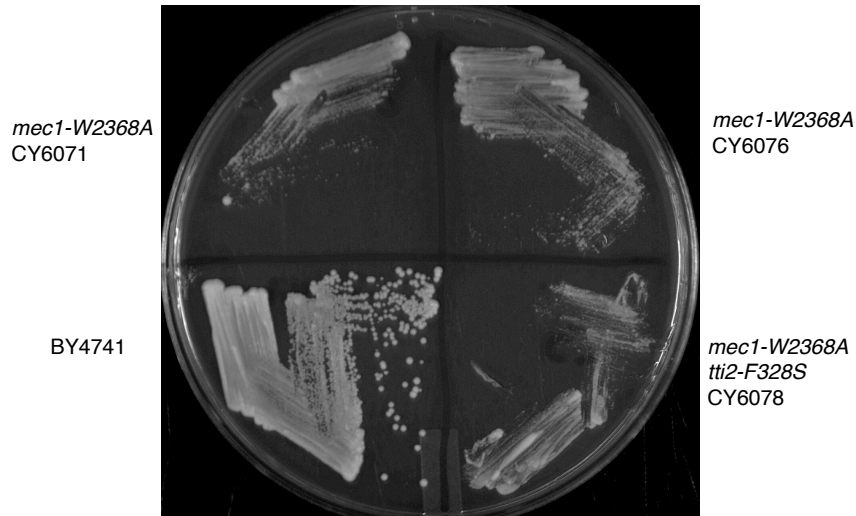
B

mec1-W2368A
CY6071

mec1-W2368A
CY6076

BY4741

mec1-W2368A
tti2-F328S
CY6078

Figure S4 *tti2-F328S does not suppress the temperature sensitivity of mec1-W2368A.* A. pCB2317 for converting tryptophan 2368 of Mec1 to alanine. The altered codon is underlined. *HIS3* was inserted at the *Bam*HI site. A *Bcl*I site was placed downstream of the stop codon to identify the allele. B. *mec1-W2368A-HIS3* was integrated into a diploid strain heterozygous for *tti2-F328S* (CY6045). The*TTI2* allele of spore colonies growing on media depleted of histidine were sequenced. CY6071 and CY6072 were *TTI2*, CY6078 was *tti2-F328S*. The strains were streaked onto a YPD plate and grown at 37° for 3 days.